ARCHIVIO ISTITUZIONALE DELLA RICERCA

Alma Mater Studiorum Università di Bologna
Archivio istituzionale della ricerca

Most Ancient Evidence for Life in the Barberton Greenstone Belt: Microbial Mats and Biofabrics of the ~3.47 Ga Middle Marker Horizon

This is the final peer-reviewed author's accepted manuscript (postprint) of the following publication:

Published Version:
Keyron, H., Barbara, C., Frédéric, F., Frances, W. (2018). Most Ancient Evidence for Life in the Barberton Greenstone Belt: Microbial Mats and Biofabrics of the ~3.47 Ga Middle Marker Horizon. PRECAMBRIAN RESEARCH, 312, 45-67 [10.1016/j.precamres.2018.04.007].

Availability:
This version is available at: https://hdl.handle.net/11585/619579 since: 2021-12-01

Published:

DOI: http://doi.org/10.1016/j.precamres.2018.04.007

Terms of use:

Some rights reserved. The terms and conditions for the reuse of this version of the manuscript are specified in the publishing policy. For all terms of use and more information see the publisher's website.

This item was downloaded from IRIS Università di Bologna (https://cris.unibo.it/).
When citing, please refer to the published version.

(Article begins on next page)

08 October 2026

This is the final peer-reviewed accepted manuscript of

Keyron Hickman-Lewis; Barbara Cavalazzi; Frédéric Foucher; Frances Westall: Most Ancient Evidence for Life in the Barberton Greenstone Belt: Microbial Mats and Biofabrics of the ~3.47 Ga Middle Marker Horizon. PRECAMBRIAN RESEARCH, 312. 0301-9268

DOI: 10.1016/j.precamres.2018.04.007

The final published version is available online at:
http://dx.doi.org/10.1016/j.precamres.2018.04.007

Rights / License:

The terms and conditions for the reuse of this version of the manuscript are specified in the publishing policy. For all terms of use and more information see the publisher's website.

This item was downloaded from IRIS Università di Bologna (https://cris.unibo.it/)

When citing, please refer to the published version.

Most ancient evidence for life in the Barberton greenstone belt: Microbial mats and biofabrics of the ~3.47 Ga Middle Marker horizon

Keyron Hickman-Lewis[a,b,*], Barbara Cavalazzi[b,c], Frédéric Foucher[a], Frances Westall[a]

[a] CNRS Centre de Biophysique Moléculaire (CBM), Rue Charles Sadron, 45071 Orléans, France
[b] Dipartimento di Scienze Biologiche, Geologiche e Ambientali (BiGeA), Università di Bologna, Via Zamboni 67, 40126 Bologna, Italy
[c] Department of Geology, University of Johannesburg, PO Box 524, Auckland Park 2006, Johannesburg, South Africa

ARTICLE INFO

Keywords:
Archaean
Early life
Microbial mats
Barberton greenstone belt
Middle Marker
Biogenicity

ABSTRACT

The Middle Marker – horizon H1 of the Hooggenoeg Formation – is the oldest sedimentary horizon in the Barberton greenstone belt and one of the oldest sedimentary horizons on Earth. Herein, we describe a range of carbonaceous microstructures in this unit which bear resemblance to phototrophic microbial biofilms, biosedimentary structures, and interpreted microfossils in contemporaneous greenstone belts from the Early Archaean. Post-depositional iron-rich fluid cycling through these sediments has resulted in the precipitation of pseudo-laminated structures, which also bear resemblance, at the micron-scale, to certain microbial mat-like structures, although are certainly abiogenic. Poor preservation of multiple putative microbial horizons due to coarse volcaniclastic sedimentation and synsedimentary fragmentation by hydrothermal fluid also makes a conclusive assessment of biogenicity challenging. Nonetheless, several laminated morphologies within volcaniclastic sandstones and siltstones and coarse-grained volcaniclastic sandstones are recognisable as syngenetic photosynthetic microbial biofilms and microbially induced sedimentary structures; therefore, the Middle Marker preserves the oldest evidence for life in the Barberton greenstone belt. Among these biosignatures are fine, crinkly, micro-tufted, laminated microbial mats, pseudo-tufted laminations and wisp-like carbonaceous fragments interpreted as either partially formed biofilms or their erosional products. In the same sediments, lenticular objects, which have previously been interpreted as *bona fide* microfossils, are rare but recurrent finds whose biogenicity we question. The Middle Marker preserves an ancient record of epibenthic microbial communities flourishing, struggling and perishing in parallel with a waning volcanic cycle, an environment upon which they depended and through which they endured. Direct comparisons can be made between environment-level characters of the Middle Marker and other Early Archaean cherts, suggesting that shallow-water, platformal, volcanogenic-hydrothermal biocoenoses were major microbial habitats throughout the Archaean.

1. Introduction

The Barberton greenstone belt, within the Kaapvaal Craton (Fig. 1), is one of several ancient sequences that provides a window into sedimentary depositional environments of the early Earth. Together with the Pilbara, it is one of only two well preserved palaeontological en claves from which remnants of ancient bacterial life have been con vincingly described (Wacey, 2009; Westall, 2016; Hickman Lewis et al., accepted). Its stratigraphy has been examined in detail by Lowe and Byerly (1999, 2007) and Hofmann (2011). Claims of varying validity for ancient life have included microbial fossils and organic remains (Barghoorn and Schopf, 1966; Pflug, 1966; Engel et al. 1968; Nagy and Nagy, 1969; Muir and Grant, 1976; Knoll and Barghoorn, 1977; Walsh and Lowe, 1985; Walsh, 1992; Westall and Gernecke, 1998; Westall et al., 2001, 2006, 2015; Javaux et al., 2010; Homann et al., 2016; Oehler et al., 2017; Kremer and Kazmierczak, 2017), microbial edifices such as stromatolites (Buick et al., 1981; Byerly et al., 1986; Walsh and Westall, 2003), microbial mats or microbially induced sedimentary structures (Walsh, 1992; Walsh and Lowe, 1999; Tice and Lowe, 2004, 2006; Tice et al., 2004; Westall et al., 2006, 2011, 2015; Noffke et al., 2006a,b; Tice, 2009; Heubeck, 2009; Gamper et al., 2012; Homann et al., 2015), and lava hosted microtubules (Furnes et al., 2004, 2007; Banerjee et al., 2006). As with most examples of putative ancient life, the substantial weight of the burden of proof (Westall and Cavalazzi, 2011; Brasier et al., 2011), together with the lack of a 'smoking gun' due to the predicament of long term preservation (Tice and Lowe, 2006) means that most of these claims have faced criticism (see Wacey, 2009, for a recapitulation of many such claims and refutations).

* Corresponding author at: CNRS Centre de Biophysique Moléculaire (CBM), Rue Charles Sadron, 45071 Orléans, France.
E-mail address: keyron.hickman-lewis@cnrs-orleans.fr (K. Hickman-Lewis).

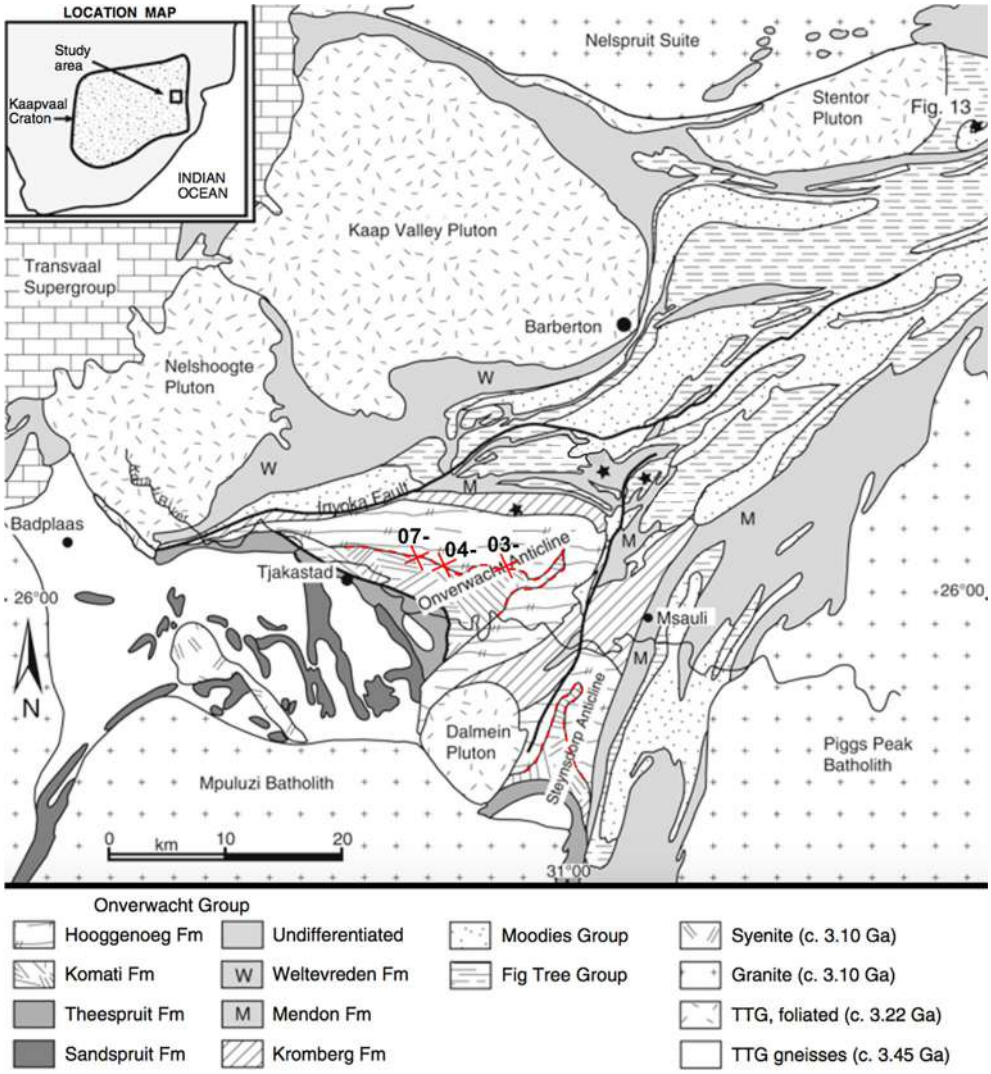

Fig. 1. Geological map of the Barberton Greenstone Belt; inset shows location within the Kaapvaal craton. The Middle Marker (dashed red lines) outcrops through the Onverwacht and Steynsdorp anticlines at the contact zone of the Komati and Hooggenoeg formations. Study areas are marked with red crosses. Modified from Hofmann (2005). (For interpretation of the references to colour in this figure legend, the reader is referred to the web version of this article.)

1.1. Geological setting

The Middle Marker horizon is the sedimentary unit defining the base of the Hooggenoeg Formation in the Onverwacht Group (Fig. 2; Viljoen and Viljoen, 1969). It is thus the oldest identified sedimentary horizon in the Barberton greenstone belt. Detrital zircon dating yields an age, *terminus post quem*, of 3.472 ± 0.005 Ga (Armstrong et al., 1990), which may be taken as accurate, and not an overestimation, since much of the underlying crust of the Kaapvaal craton appears to be little older (Drabon et al., 2017). Additionally, felsic material in the Middle Marker is a likely source rock for common zircons (Hofmann et al., 2013). The Middle Marker is a 3 6 m thick layer consisting of mostly silicified current deposited volcaniclastic material, and black chert which possibly results from the silicification of a non volcanic protolith (Lanier and Lowe, 1982). In a previous sedimento logical study of this horizon, Lanier and Lowe (1982) deduced a deposi tional environment involving a cone flanking, prograding sedimentary platform, in which volcaniclastic sediments were deposited from a waning subaerial volcanic system, in a basin isolated from continental terranes. Although energetic, basin wide tidal activity was minor, local current and wave driven subaqueous deposition has been noted, and a subtidal en vironment is implied for those parts of the sequence. A significant felsic component suggests that this chert represents a waning cycle of volcanism between two pulses of mafic magmatic activity (Viljoen and Viljoen, 1969; Lanier and Lowe, 1982), although Lowe (1999a,b) notes that Al_2O_3, Zr, TiO_2 and Cr ratios (*i.e.* the immobile elements) unambiguously document the simultaneous input of komatiitic ashes. Hofmann et al. (2013) further note that while elevated Gd_N/Yb_N and La_N/Sm_N indicate felsic contributions, komatiitic ashes are a common constituent in the unit.

1.2. Sedimentology of the Middle Marker horizon

Having undergone no greater than lowest greenschist metamorphism (Hurley et al., 1972; Lanier and Lowe, 1982; Bourbin et al., 2013; Delarue et al., 2016), primary sedimentary textures and geochemical signatures from the Middle Marker are relatively well preserved. Since it is the oldest sedimentary horizon in the Barberton greenstone belt and one of the oldest sedimentary horizons on Earth, it provides a particularly pertinent insight into ancient volcaniclastic settings. Lanier and Lowe (1982) demarcated the chert into three stratigraphic divisions lower, middle, and upper (Fig. 3) which are here summarised.

The lower unit consists of thinly laminated grey black chert deposited atop a pillowed, mafic volcanic substrate, and features interstratified, cross laminated, fine to medium grained volcaniclastics. The abundance and grain size of these volcaniclasts increase upward in the lower unit. Light and dark couplets define thin horizontal and lenticular laminations. Other se dimentary structures, such as ripples, flaser bedding and high angle micro-

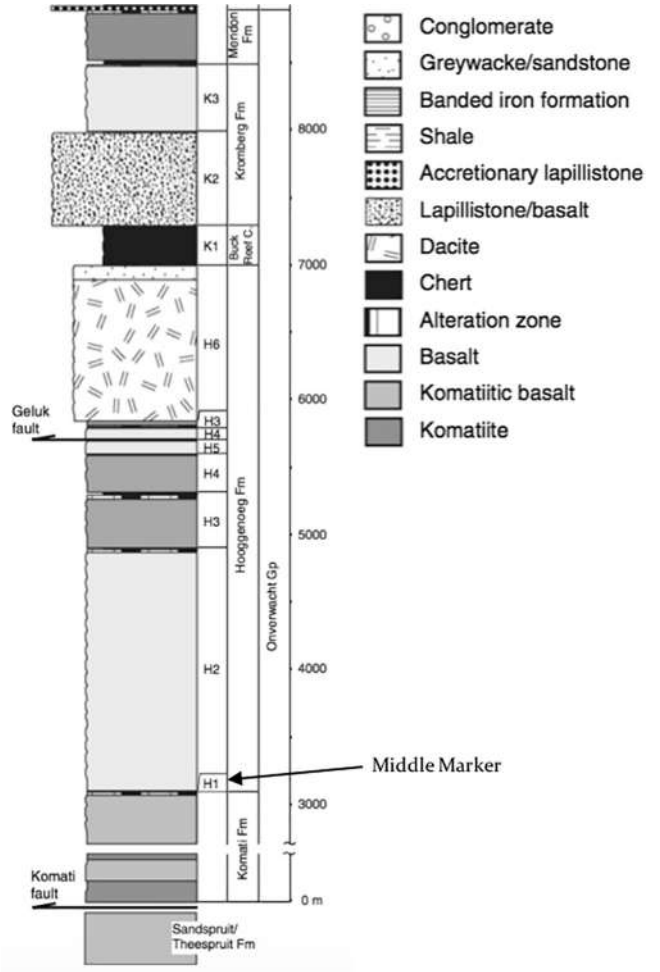

Fig. 2. Stratigraphic column depicting the Onverwacht Group from the western limb of the Onverwacht anticline, indicating the position of the Middle Marker. Adapted from Hofmann (2011).

scale cross bedding, are taken as indicative of entirely submarine, low energy deposition in shallow water, alternating between traction and sus pension sedimentation (Reineck, 1967; Paris et al., 1985; Lanier and Lowe, 1982). Soft sediment deformation, such as lenticular load structures, are also common. Flaser bedding, together with accretionary lapilli, suggest an in creasing influence of volcanism upward in the strata. Our study also notes geochemical and textural evidence for diffuse hydrothermal like infiltration through laminated volcaniclastic sandstones and siltstones which, where most intense, disrupts original sedimentary features (*cf.* Paris et al., 1985; Hofmann, 2011).

The middle section is dominantly even bedded, coarser grained volcaniclastic material weathered green to buff in colour, which contains many accretionary lapilli (Lowe and Knauth, 1978; Lowe and Byerly, 2007). The protolith contains crystal, vitreous and lithic components from volcanic sources (Lanier and Lowe, 1982). Sedimentary structures include trough bedding and tabular cross stratification of volcaniclastic sandstone, separated by minor chert layers. Trough scours contain fine grained sediments with interpreted wave ripple cross lamination (Lanier and Lowe, 1982; Lowe and Byerly, 1999). Ripped up clasts of grey black chert from the underlying layers are common in the overlying layers of volcaniclastic detritus. The middle section therefore depicts the shoaling of water concomitant with an increase of coarse sediment supply and high energy currents.

Finally, the upper unit is composed mostly of fine grained grey black chert with local thin beds of volcaniclastics and conglomeratic rocks. This chert is massive and poorly stratified, although small scale sedimentary structures, such as fine laminations and cross stratification, together with relict fine clastic textures, suggest that the protolith was detrital (Lanier and Lowe, 1982). The upper unit therefore represents a fine grained airfall deposit, the conclusion of waning volcanism, into a low energy, subaqueous basin. The co occurrence of pyrite and gypsum, the latter pseudomorphed, denotes deposition in anoxic conditions (Siesser and Rogers, 1976, Lanier and Lowe, 1982) at warm temperatures of up to 52 58 °C, concurrent with calculated contemporaneous ocean temperatures from alternative proxies (Knauth, 2005; Tartèse et al., 2017). Chert conglomerate is found in the upper reaches of the Middle Marker, which mixes grey chert and volcaniclastic detritus in what is interpreted as a combination of cracking and current reworking of the sediment (Lanier and Lowe, 1982). Desiccation cracks at the top of the grey chert suggest some subaerial exposure, and thus the sequence is broadly aligned with an intertidal supratidal flat environ ment.

In what follows, we describe and evaluate the biogenicity of previously unrecognised putative microbial mat fabrics, microbially induced sedimentary structures and microfossil like objects within the Middle Marker horizon. Some of these features may represent the most ancient evidence for microbial life in the Barberton region, and the second oldest convincing evidence for life on Earth.

2. Materials and Methods

All samples studied come from outcrops of the horizon on the western limb of the Onverwacht anticline, which is the least metamorphosed section of Middle Marker outcrop (Fig. 1). By contrast, the Middle Marker of the Steynsdorp anticline has undergone a greater degree of thermal metamorphism, and is characterised by a coarsened quartz matrix, while that of the eastern limb of the Onverwacht anticline is highly metamorphosed, with most original textural features destroyed (Lanier and Lowe, 1982).

Samples were collected during field campaigns in 2003, 2004 and 2007 (Table 1). All sample collection localities can be readily relocated by means of their co ordinates in Global Positioning Systems (G.P.S.). Samples are stored at the CNRS Centre de Biophysique Moléculaire (CBM), Orléans. Methods are described in full in the Supplementary Materials.

3. Results I lithofacies

3.1. Lithofacies

Petrographic analyses separate the studied samples into three distinct lithofacies: (i) coarse felsic volcaniclastic sandstone, having angular grains up to 3 mm in size, including accretionary lapilli, with weak, macro scale cross bedding (Fig. 4A C); (ii) massive black chert rich in organic carbon, hereafter termed clotted carbonaceous chert (after Lowe and Knauth, 1977), composed of angular or sub rounded particles of organic carbon up to 2 mm diameter either suspended in a silica matrix or in grain supported textures, with silica replaced rounded particles (Fig. 4D,E); and (iii) lami nated, green grey, volcaniclastic sandstone siltstone, having millimetre scale alterations between volcaniclastic rich layers and grey black cherti fied layers rich in organic carbon (Fig. 4F H). Massive black clotted carbonaceous cherts appear homogeneous in hand specimen, coarse volcaniclastic sandstones are yellow brown and faintly stratified, while laminated sandstones and siltstones are green grey in colour and stratified by dark planar and crinkly laminations.

3.1.1. Facies 1: Coarse volcaniclastic sandstone

The volcaniclastic fraction (> 70%) is composed of poorly sorted volcanic glass, randomly distributed mafic and felsic minerals, and lithic fragments (Fig. 4A,B). Some samples are dominantly accretionary lapilli (Fig. 4C). Their mineralogy is dominantly altered feldspars and amphiboles (likely hornblende), angular shards of volcanic glass, minerals with yellow pleochroism, that are possibly sericitised feldspar (*cf.* Hurley et al., 1972), together with pyrite and very minor oxides. SEM EDS reveals a relict Fe Mg richness in certain zones, which corroborates mafic input (Lowe, 1999a,b;

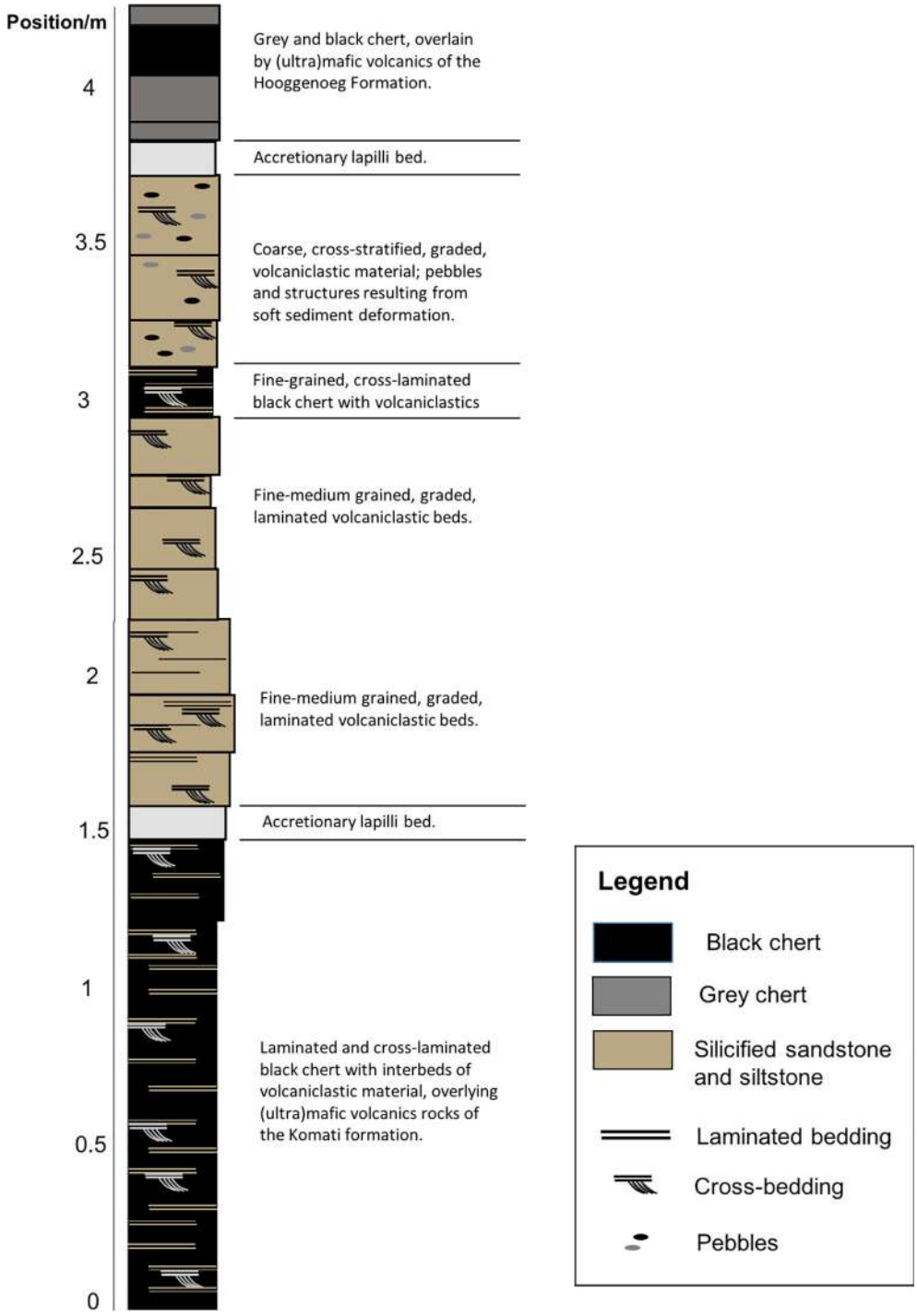

Fig. 3. Generalised stratigraphic column of the Middle Marker from the western limb of the Onverwacht anticline. Adapted from, and annotated after, Lanier and Lowe (1982).

Hofmann et al., 2013), however, these minerals show widespread alteration to sericite, chlorite and Fe Al bearing minerals (Hurley et al., 1972) has occurred (Figs. 5 7). Cr indicates Cr spinel (chromite), a mineral which is usually resistant to silicification (Cr in Fig. 6B). Raman spectroscopy identified dispersed anatase and rutile within an overwhelmingly silica matrix. This matrix is characterised by a yellow orange, web like alteration texture (Fig. 4B). Fine grained silica has pervasively replaced many components and obfuscates the original mineralogy, such that mineralogical identifications are often necessarily made on crystal habit alone. Basaltic rocks, particularly volcanic glass, alter extremely rapidly to produce a thin phyllosilicate alteration layer; this has been extensively experimentally demonstrated (Oelkers and Gíslaison, 2001; Gíslason and Oelkers, 2003; Wolff Boenisch et al., 2006; Westall et al., 2018) and is apparent from the Al-rich composition of the groundmass. In Early Archaean sediments, the edges of volcanic glass shards are often outlined by anatase, whereas muscovite and stilpnomelane (see spectra in Fig. 7) can result from po tassium metasomatism. The high feldspar content of the volcaniclastics suggests a significant input from felsic pyroclastic material, whereas their poor sorting and angular grain morphology suggests a proximal eruption, after which negligible transportation and reworking of the sediment has occurred. Perceptible imbrication in some layers suggests local, albeit weak, currents (Fig. 4A).

Table 1
Sample details.

Sample	Location	Classification	Description and specific characteristics
03SA01	S 25°58′47″ E 30°53′91,7″	Coarse-grained volcaniclastic sandstone	Coarse, angular volcaniclasts within silica matrix. Rare carbonaceous laminations. Relatively high feldspathic content. Well-bedded, some graded bedding. Widespread alteration of particles, forming Fe-rich coatings.
03SA02	S 25°58′47″ E 30°53′91,7″	Coarse-grained volcaniclastic sandstone with subordinate interbeds of laminated black chert	
03SA03	S 25°58′47″ E 30°53′91,7″	Coarse-grained volcaniclastic sandstone	Coarse, angular volcaniclastics and a large volume of accretionary lapilli interbedded with thin carbonaceous laminations. Well-bedded, some graded bedding. Widespread alteration of particles, forming Fe-rich coatings.
04SA12A	S 25°58.434′ E 30°55.592′	Laminated sedimentary black chert	
04SA12B	S 25°58.434′ E 30°55.592′	Coarse laminated sedimentary black chert	Frequent carbonaceous laminations in graded bedding sequences. Coarser grain size results in poorer preservation of carbonaceous fabrics.
04SA12C	S 25°58.434′ E 30°55.592′	Massive black chert; contact with overlying coarse volcaniclastic sandstone	
04SA14	S 25°58.426′ E 30°55.357′	Laminated volcaniclastic sandstone and siltstone	
04SA16	S 25°58.438′ E 30°55.616′	Coarse laminated sedimentary black chert	
07SA21A	S 25°58′12,8″ E 30°53′04,0″	Laminated volcaniclastic sandstone and siltstone	Fine-medium silicified volcaniclastic sandstone with regular carbonaceous laminations. Angular clasts with a general trend of upward coarsening leading to repeated couplets of volcaniclastics and carbonaceous laminations.
07SA21B	S 25°58′12,8″ E 30°53′04,0″	Laminated volcaniclastic sandstone and siltstone	
07SA22	S 25°58′12,8″ E 30°53′04,0″	Massive, clotted black chert	Angular carbonaceous clots in a matrix-supported rock.
07SA23A	S 25°58′12,8″ E 30°53′04,0″	Coarse volcanic detritus with regions of volcaniclastic sandstone	Very coarse volcanic particles substantially altered to sericite, illite, chlorite and other phyllosilicates, surrounded by a silica matrix.
07SA23B	S 25°58′12,8″ E 30°53′04,0″	Laminated volcaniclastic sandstone and siltstone	Medium-coarse volcanic material and volcaniclasts interbedded with regular carbonaceous laminations. Some reverse graded bedding; carbonaceous laminations usually overlain by very coarse, substantially altered volcanic material.
07SA24	S 25°58′12,8″ E 30°53′04,0″	Massive, clotted black chert	Carbonaceous clots form a grain-supported texture together with rounded silica-replaced grains. Frequent cross-cutting microquartz veins.
07SA25	S 25°58′12,8″ E 30°53′04,0″	Massive, clotted black chert	Well-rounded carbonaceous particles form a grain-supported texture together with rounded silica-replaced grains. Frequent cross-cutting microquartz veins.

A pervasive web like alteration texture fills pore space and coats grains (Fig. 4B). It bifurcates and anastomoses irregularly, but follows exactly the grain margins. In void spaces between grains, the laminations are ‘connected’ by a web like fabric.

3.1.2. Facies 2: Clotted carbonaceous chert

Clotted carbonaceous chert (cf. Lowe and Knauth, 1977; Hickman Lewis et al., 2016) is a chert rich in organic, kerogen like carbonaceous material. Such massive, silicified rocks consist of carbonaceous ‘clots’, which may be either well rounded or irregular (see Fig. 4D,E), within a silica matrix (*cf.* Facies C of the Josefsdal Chert, Westall et al., 2015). In hand sample and thin section, these cherts appear matt black, with in frequent layering (Fig. 4D). The spatial interrelationship between silica and carbon gives the chert its characteristic millmetre scale ‘clotted’ texture.

Clotted carbonaceous cherts include ~50% medium coarse sand grade, carbonaceous particles (Figs. 4D,E and 8): this comprises 70% angular composite particles, > 25% angular simple particles and < 5% flakes and wisps (*cf.* Walsh and Lowe, 1999; Hickman Lewis et al., 2016). Aside from carbonaceous matter, this lithofacies contains ~ 45% microcrystalline silica (Figs. 4D,E and 8B) and 5% dispersed volcanogenic material, indicated by the proxy mineral anatase (Fig. 8B). Composite carbonaceous particles are constructed of hundreds of sub angular simple carbonaceous particles (*cf.* Greco et al., 2018). Wisps of carbon, though bearing superficial semblance to bio genic roll up structures (Walsh and Westall, 2003; Tice and Lowe, 2004), clearly follow the boundaries of sub angular grains.

3.1.3. Facies 3: Laminated, green grey volcaniclastic sandstone siltstone

Laminated sandstone siltstones are the most texturally diverse of the three lithofacies. They consist of volcaniclastic and volcanic components equivalent to coarse volcaniclastic sandstones, with grains sizes of 0.1 2 mm, and are laminated on the millimetre to centimetre scale (Fig. 4F H). The matrix contains detrital mafic and felsic minerals, including altered pyroxene (diopside augite), plagioclase, amphiboles, silicified volcaniclastics altered to phyllosilicate mineralogies, and prismatic minerals which EDS point analyses identify as chlorite and Fe Al phyllosilicates (Fig. 7; Hurley et al., 1972). The green grey colour of this lithofacies is imparted by extensive chlorite alteration. Raman analyses of the lithofacies identify dispersed siderite and anatase particles, often associated with organic matter. Layers of volcanogenic sediments are invariably topped by multi laminar organic carbon rich laminations (Fig. 4F). By contrast to the other lithofacies, evidence for current induced sedimentation is relatively common: cross stratification, well sorted layers, surficial sediment deformation features and imbricated clasts are present, all of which necessitate at least local, weak current activity (see also Lanier and Lowe, 1982).

Laminated fabrics rich in organic carbon are frequent features of the micro stratigraphy, occurring every 1 10 mm, and are morphologically diverse (Figs. 4 and 7). Most are crinkly and continuous over the scale of tens of centimetres in samples (Fig. 4F) although others are flat lying and undulatory (Fig. 4H). They are conformable with the sedimentary sequence and therefore primary fabrics. In contrast to the coarse volcaniclastic sandstones and clotted carbonaceous cherts, organic carbon is a volumetrically significant component of this lithofacies: it occurs predictably, recurrently and identically at the centimetre scale.

3.1.4. Geochemical indications of palaeoenvironment

Major and trace element data gathered from ‘bulk’ hand sample analysis can shed light on the palaeoenvironmental and chemical oceano graphic conditions of deposition (see Grassineau et al., 2002; Gourcerol et al., 2015, 2016). Representative samples of each of the three lithofacies heretofore identified (coarse volcaniclastic sandstone, 03SA01; clotted

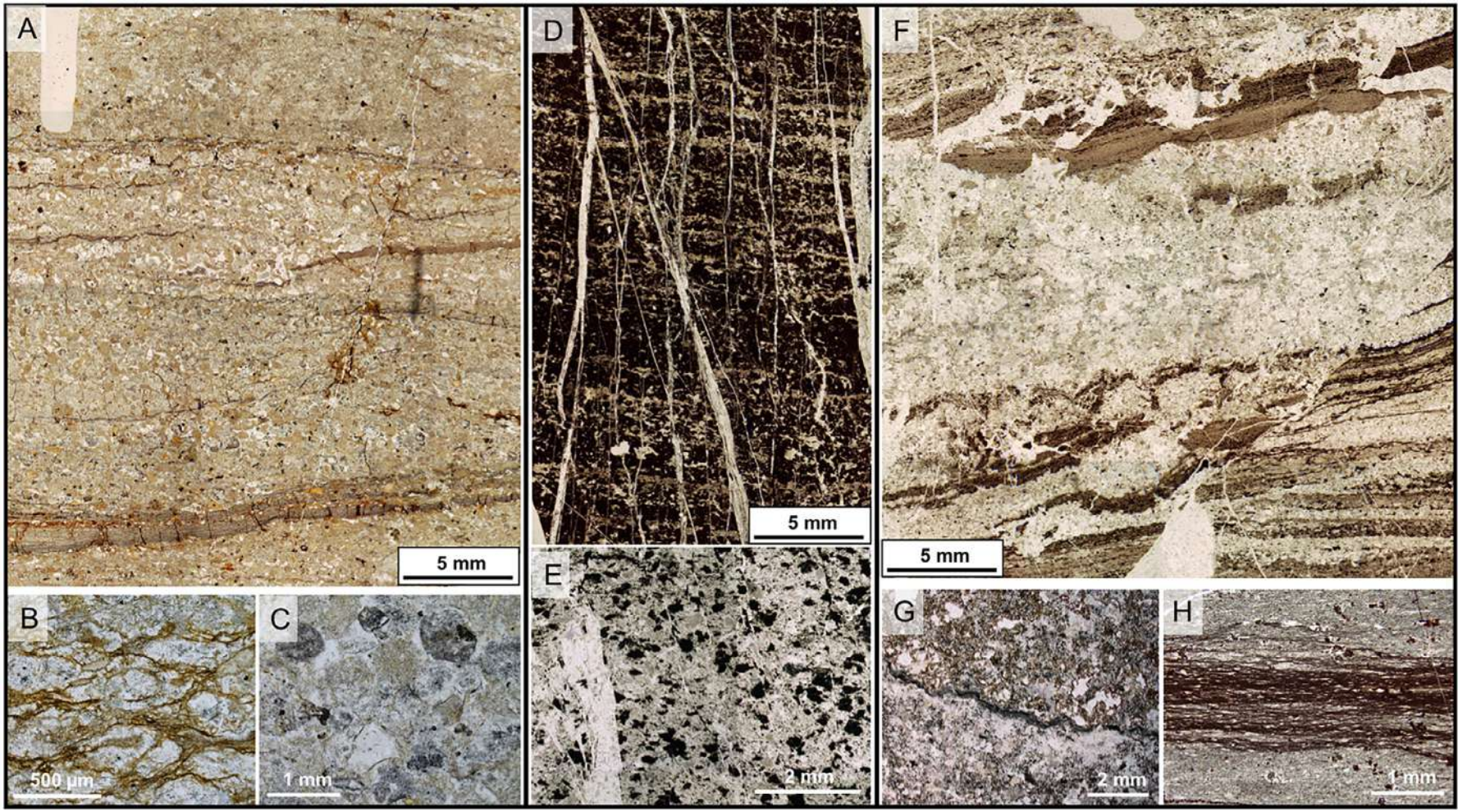

Fig. 4. Atlas of the three major lithofacies in the Middle Marker. (A–C) Thin section mosaic of coarse-grained volcaniclastic sandstones, cross-bedded on the macro-scale. (A) Thin section scan of volcaniclastic sandstone 03SA03. (B) Photomicrograph of 03SA01, showing the yellow-brown, web-like fabric which pervades all void spaces. (C) Accretionary lapilli. (D and E) Massive, black, clotted carbonaceous chert. (D) Thin section mosaic of 07SA25, clotted carbonaceous chert with sub-rounded clots and flakes, interspersed with rounded quartz grains and microcrystalline matrix. The section is cross-cut and interbedded with vertical and stratiform microquartz and coarse quartz veins. (E) Photomicrograph of 07SA22, showing irregular, spiky, carbonaceous clots intermixed with siliceous particles. (F–H) Laminated volcaniclastic sandstones and siltstones. (F) Thin section mosaic of laminated crinkly carbonaceous fabrics interbedded with graded volcaniclastic deposits, bearing the hallmarks of deposition in a shallow marine environment. (G) Crinkly-wavy, thick, carbonaceous lamination overlain by volcaniclastic detritus. (H) Low-relief, crinkly lamination, incorporating oriented quartz grains, in volcaniclastic siltstone. (For interpretation of the references to colour in this figure legend, the reader is referred to the web version of this article.)

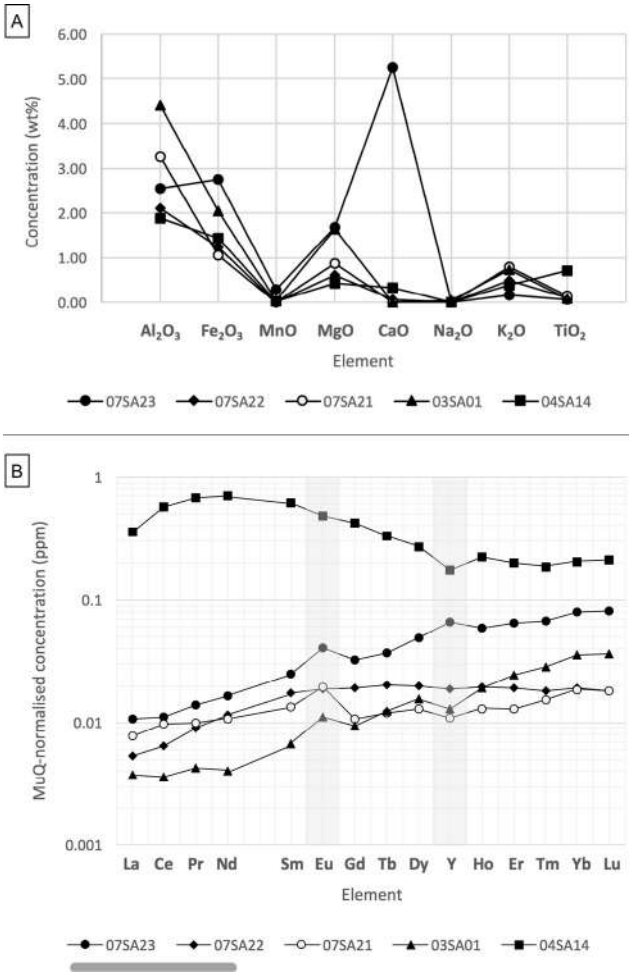

Fig. 5. Bulk geochemical characterisation of several of the samples used in the study, using representative samples of the three lithofacies (see Fig. 4, Table 1). A) Major element concentrations. B) REE + Y plots normalised to Mud from Queensland (MuQ; Kamber et al., 2005). The generally incremental positive trend indicates a dominant seawater component, whereas the weakly positive Euanomaly indicates a minor component from hydrothermal fluid. The trend of 04SA14 is very much the inverse of the other samples, and shows remarkably heightened REE + Y concentrations; this effect has been attributed to post-diagenetic alteration, and therefore this sample is likely uninformative of the depositional setting of the unit.

carbonaceous chert, 07SA22; and laminated volcaniclastic sandstone and siltstone; 07SA21, 07SA23, 04SA14) were analysed by ICP OES and ICP MS. Most samples show a bulk composition consistent with a mostly altered mafic and minor felsic precursor (high Al, Fe, Mg, K content) whereas one sample, 07SA23, shows a remarkably high Ca content (Fig. 5A). This is consistent with an observed 9 wt% calcite content in this sample (X ray diffraction, results not shown).

Rare earth element plus yttrium (REE + Y) analyses normalised to Mud from Queensland (MuQ, *cf*. Kamber et al., 2005) of the same samples show with the notable exception of sample 04SA14 a generally increasing trend from light rare earth elements (LREEs) to heavy rare earth elements (HREEs). Two of the samples of laminated volcaniclastic sandstone and siltstone (07SA21, 07SA23) and the sample of coarse volcaniclastic sandstone (03SA01) show pronounced positive Euanomalies, one of which also shows a weakly positive Y anomaly (Fig. 5B). 04SA14 shows almost the inverse of this trend, and much higher concentrations of REE + Y. By contrast, the sample of clotted carbonaceous chert shows a largely flat REE + Y trend.

4. Results II laminated fabrics and carbonaceous microstructures

4.1. Fine, crinkly, micro tufted laminations

Fine, crinkly, often micro tufted laminations (Figs. 9A C, 10 12), occurring in packets of thickness from 200 μm to 2.5 mm, are the most common carbonaceous laminated feature in the Middle Marker. They have a gross structure composed of fine, non isopachous sets of laminae which drape and bind detrital quartz and volcanogenic grains, and are inter calated with silica lenses and layers (Figs. 10 and 11B E). Single laminae exhibit bifurcation and anastomosis. The entrained, oriented grains have identical chemistry to the groundmass, *i.e.* Fe Mg Al K mafic and felsic particles (Fig. 12E,F). Lamina packets generally mantle sedimentary layers (Fig. 10A,B) and frequently drape grains which are oriented parallel to their laminae (Figs. 10 and 11C E). Surficial relief is low, generally below 100 μm, and, where present, occurs as microscopic tufts (Figs. 9A and 10A,B). Tufts manifest themselves at regular intervals (every several tens of microns laterally), and with greater regularity when on inclined stratifi cation. At low magnification, crinkly laminations appear continuous over tens of centimetres, however, they are in fact constructed of many shorter film like objects of 50 300 μm in length (Fig. 11C E). They exhibit ductile response to microfaults, intrusions and loading (Fig. 11).

The compression of crinkly, laminated layers is laterally heterogeneous. Where compressed, little of the original voluminous fabric is preserved; instead, these features are preserved as faintly laminated carbonaceous layers within which quartz grains 'float' without grain to grain contact (Fig. 10D,E). In the matrices immediately above each laminated horizon are multiple wisp like and lenticular objects which are possibly eroded and reworked fragments of the lamination itself (see Section 4.4). Additionally, some crinkly laminae appear to have been splintered in a brittle fashion, or frayed (see Section 4.4). In the latter case, eroded fragments, again in cluding wisps and flakes, are common in the immediate vicinity.

Every crinkly laminated layer is abruptly overlain by a deposit of coarse, angular, poorly sorted volcanic and volcaniclastic detritus, often glassy or tephra dominated, which appears to have been deposited rapidly, therein immediately changing the regime to deposition (Figs. 10 and 11). Ergo, crinkly laminations develop during erosional regimes, and their formation is halted during depositional regimes.

4.2. Pseudo tufted laminations

Tufted laminations are particularly thick (up to 2.5 mm) carbonac eous layers (Figs. 13 and 14). They comprise a mixture of wiry, crinkly, filament like laminations (identical to those described in Section 4.1.) admixed with microgranular material, and the scale of relief exhibited by individual tufts is an order of magnitude greater than those of crinkly laminations.

The microstratigraphy of each tufted layer is tripartite: lower regions with a chaotic mixture of elongate carbonaceous flakes (cf. Schieber et al., 2007; Noffke, 2010; Harazim et al., 2013; Hickman Lewis et al., 2016) and varied simple particles including clots of carbon; middle regions of crinkly, filament like laminae entraining medium sized sand grade particles and exhibiting anastomosis; and an upper region of tufts (Figs. 13A D and 14). Microgranular material is concentrated in the upper regions of the tufts and intermingled with laminations at the base of the layers. Tufts have a relief of up to 0.8 mm, a basal width of up to 1.2 mm, and occur at regular intervals along the lamination. The filament like laminations that constitute the base often inflect upward into the tufts (see interpretative dia grams in Fig. 13C,D), though some rare tufts fail to preserve any lamina tions within their upper reaches (Fig. 14A). Some less well preserved carbonaceous laminations resemble degraded examples of tufted lamina tions. (Fig. 14E,F) The troughs connecting tufts are often associated with dense grains settled out of deposition, demonstrating that tufts were the result of plastic deformation, thus we term these structures 'pseudo tufted' laminations.

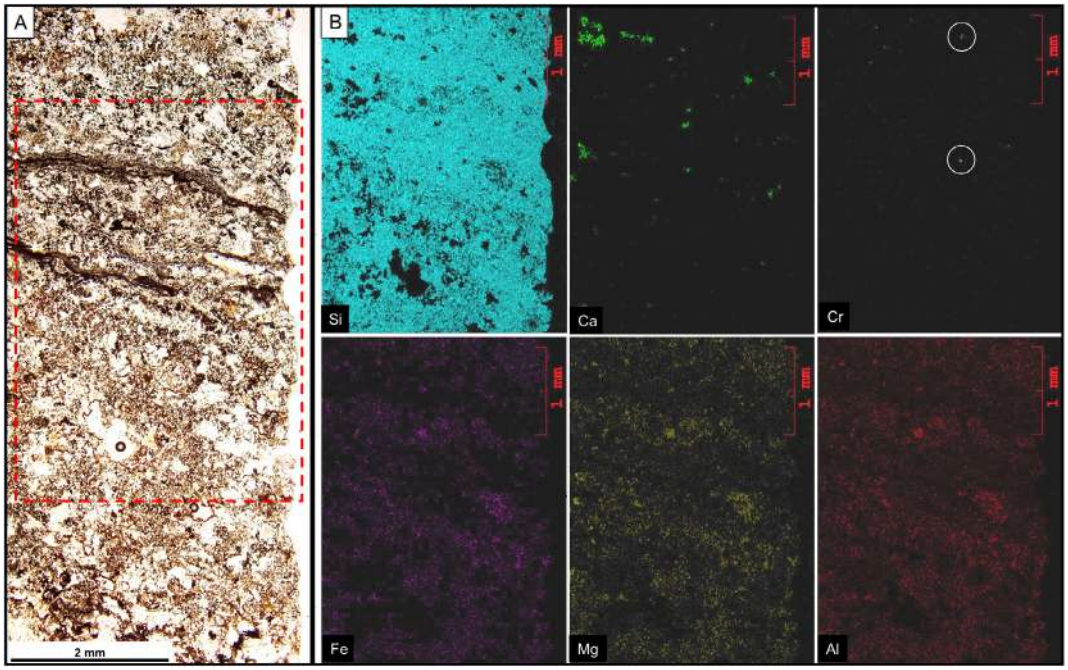

Fig. 6. SEM-EDX analyses of volcaniclastic material. (A) Buff-brown-green coarse volcaniclastic sandstone with carbonaceous laminations. Red box indicates the region of the element maps. (B) Element maps for silicon, calcium, chromium, iron, magnesium and aluminium show a broad mixture of mafic (Fe-Mg) and felsic (Ca-Al) mineralogy. Co-occurrence of Fe-Mg-Al signifies the alteration of volcanic glass and crystals to chlorite and/or smectite. In D) chromite spinel grains (unsilicified) are circled. Note the anticorrelation of silica with carbonaceous material. (For interpretation of the references to colour in this figure legend, the reader is referred to the web version of this article.)

4.3. Wisps, flakes and roll up structures

Carbonaceous wisps (cf. Walsh and Lowe, 1999) and flakes (*cf.* Noffke, 2010; Schieber et al., 2012; Hickman Lewis et al., 2016), are commonplace throughout the sediments (Figs. 11 and 15), although rare to absent in massive clotted carbonaceous cherts. Having compo sitions and dimensions equivalent to the fine, crinkly, film like lami nations, and exhibiting the same signatures of originally plastic, cohesive behaviour (*i.e.* forming roll up structures), these microstructures are likely fragments of the crinkly laminations. Erosional processes acting at the surfaces of laminations are evidenced by the presence of tear up structures (Figs. 9B, 10E and 15A,B). A tear up structure probably represents the precursor to a wisp or flake, whereas a roll up structure, such as seen in the matrix, represents the current reworked end product of the eroded fragment of microbial mat.

4.4. Lenticular objects

Within several horizons of laminated volcaniclastic sandstones and shales, lenticular structures, formerly termed spindle like structures (cf. Walsh, 1992; Sugitani et al., 2009, 2015; Oehler et al., 2017), are either intercalated with, or are contiguous within, carbonaceous laminae (Fig. 15). These structures have a size of 30 300 μm, and are morphologically consistent with other lenticular structures throughout the matrices of the same samples, often having tapering margins and central voids (Fig. 15). Fig. 15A shows a set of frayed laminae; in the immediately ad jacent region, which is mostly volcaniclastic detritus, there are at least four such lenticular objects. That the lenticular structures within the laminae have an elongate, oriented distribution parallel to the laminae (Figs. 11D and 15B,C) suggests their syngenicity with the laminae.

In the matrix, lenticular structures occur randomly but frequently, and are likely derived from the erosion of different fine, crinkly, film like laminations. They have various compositions, spanning carbonac eous through tuffaceous to vitreous (Fig. 15E H), and exhibit a wide range of sizes and morphologies dependent upon the presence of equatorial extensions, of which there may be up to two.

5. Discussion I: Sedimentary and palaeoenvironmental setting

The Middle Marker sediments document the accumulation of volcani clastic and marine material in a sedimentary regime between two long periods of dominantly mafic volcanic activity, the Komati and Hooggenoeg formations (Anhaeusser, 1973, 1978; Lowe and Byerly, 2007). The Middle Marker horizon thus reflects the waning stage of the final volcanic episode in the Komati Formation (Lanier and Lowe, 1982). As reported in previous studies (Lanier and Lowe, 1982; Lowe, 1999a,b; Hofmann et al., 2013), volcaniclastic material is the dominant constituent. SEM EDS and ICP OES analyses document the co occurrence of mafic (Fe Mg) and felsic (Al K Si) mineral compositions, evidencing their simultaneous input (Figs. 5 7 and 12). We have not observed the large volumes of carbonates described by previous workers (Hurley et al., 1972; Condie, 1981; Tankard et al., 1982), solely rare siderite (Fig. 12B) and rare rhombic crystals which are possibly silicified carbonates (not shown). X ray diffraction (XRD) analyses of some of these samples show minor calcite (up to 9 wt%; results not shown), which seems curious in light of the 'acidic' portrayal of the Archaean world. We suggest that, although the majority of the hydrosphere would have been acidic by virtue of the high pCO_2 Archaean atmosphere, the precipitation of calcite could have been permitted in the immediate vicinity of the re surgence of hydrothermal seawater fluids, where their reaction with mafic oceanic crust necessarily produces alkaline microcosms (Kempe and Degens, 1985). Indeed, in the absence of knowing the degree of stratification of the basin in which the Middle Marker sediments were deposited, we cannot comment on the relative abundances of carbonate described in previous studies, since the propensity for its precipitation cannot be estimated.

The sedimentary structures identified evidence shallow water deposition (broadly shallowing upward through the sequence as the volcanic cone progrades), and we concur with previous estimates of up to tens of metres of water depth (Lanier and Lowe, 1982; Lowe and Byerly, 2007). Lowe and Byerly (2007) describe the Middle Marker chert as having regional extent across the Onverwacht anticline, and therefore

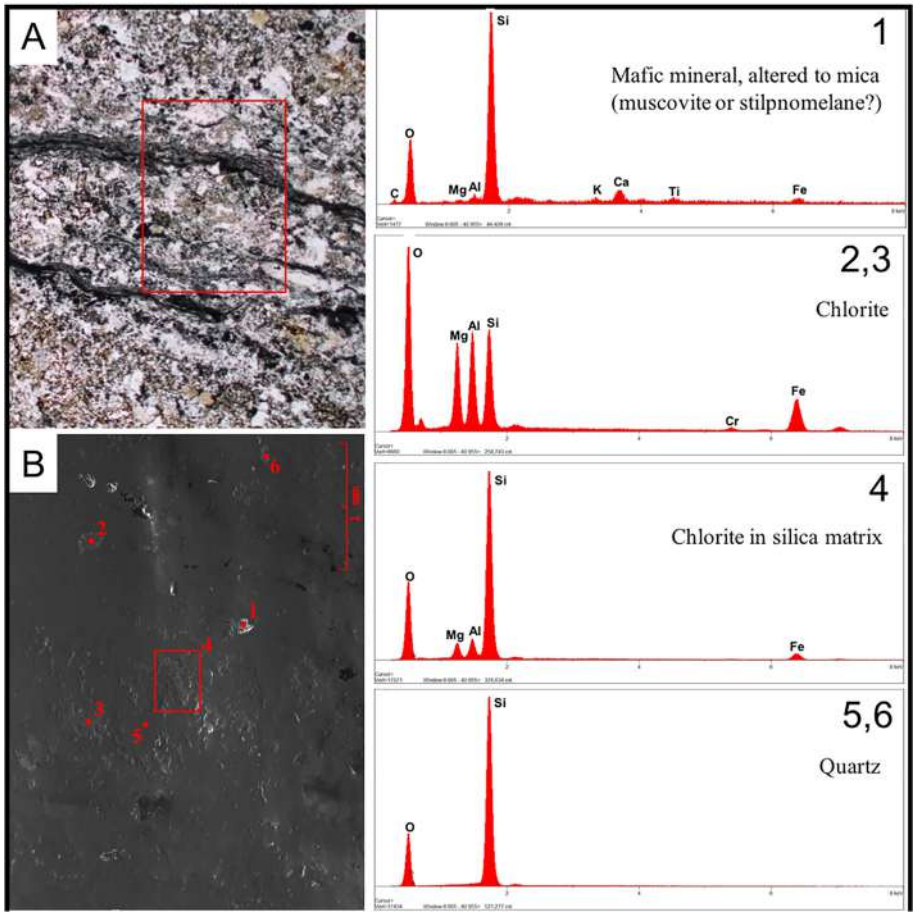

Fig. 7. SEM-EDX point analyses of volcaniclastic material. (A) Typical coarse volcaniclastic sandstone from the same region as Fig. 5. Red box indicates region of (B). (B) Points and regions analysed by SEM-EDX. Results are numbered. Broadly, the matrix is a silica-chlorite mix. (For interpretation of the references to colour in this figure legend, the reader is referred to the web version of this article.)

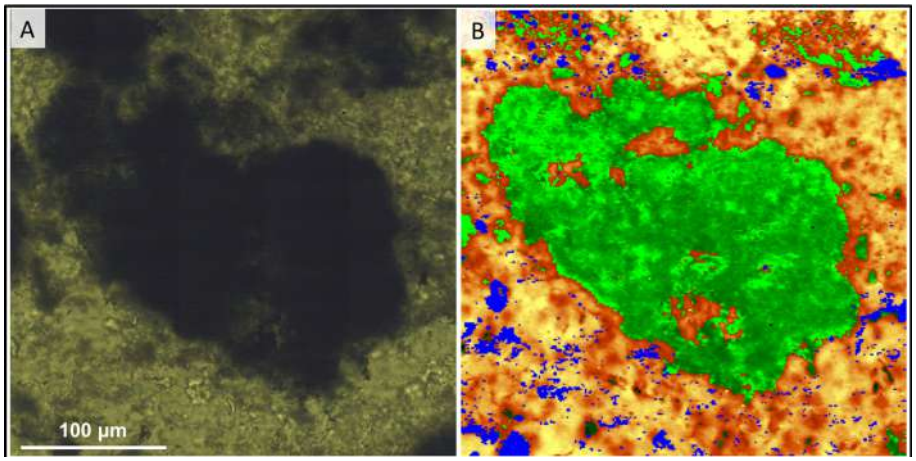

Fig. 8. Raman spectroscopic mapping of an individual clot in massive clotted carbonaceous chert. (A) Photomicrograph of clot and matrix in plane-polarised light. (B) Raman spectroscopy mapping in which carbonaceous material = green, quartz = yellow-orange, anatase = blue. (For interpretation of the references to colour in this figure legend, the reader is referred to the web version of this article.)

suggested its deposition on a flat, open, tide or wave influenced volcanic shelf. The observations herein of grain sizes varying from silt to coarse grade sand, usually in graded sequences (Fig. 4), support this view. Although sedimentary structures testify to local wave influence, there are equally periods of quiescence.

Previous reports suggested that carbonaceous material is minor and mostly occurs as either thin layers of relatively pure organic carbon rich chert and/or simple particles mixed in komatiitic ash (Hurley et al., 1972; Lowe and Byerly, 2007), however, this study, using Raman spectroscopy and SEM EDS, has unambiguously demonstrated that there are in fact a multitude of carbonaceous structures, usually occurring as laminations between cycles of volcanogenic deposits in shallow water, laminated volcaniclastic sandstones and siltstones.

The carbonaceous material shows a thermal maturity consistent with the history of the rock (Fig. 16). All spectra of carbonaceous material show pronounced D and G bands centred around 1350 cm^{-1} and 1600 cm^{-1}, respectively, and a low intensity second order signal. This implies that the carbon has low 2 D structural organisation, little to no 3 D structural ordering (Lespade et al., 1982), and is thus not graphi tised (Marshall et al., 2007). A shoulder on the D1 band between 1130 cm^{-1} and 1260 cm^{-1} is present in all types of analysed carbo naceous matter, further indicative of a low crystallinity (Sadezky et al., 2005), which has been reported from similar stratiform cherts (Sforna et al., 2014; Hickman Lewis et al., 2016).

The intensity ratio of the D and G bands (I_{D1}/I_G) and the structural disorder ratio $I_{D1}/(I_{D1} + I_G)$ correlate with the degree of structural disorder, and this can assist in environmental interpretations of the different facies of carbonaceous material in the Middle Marker. In

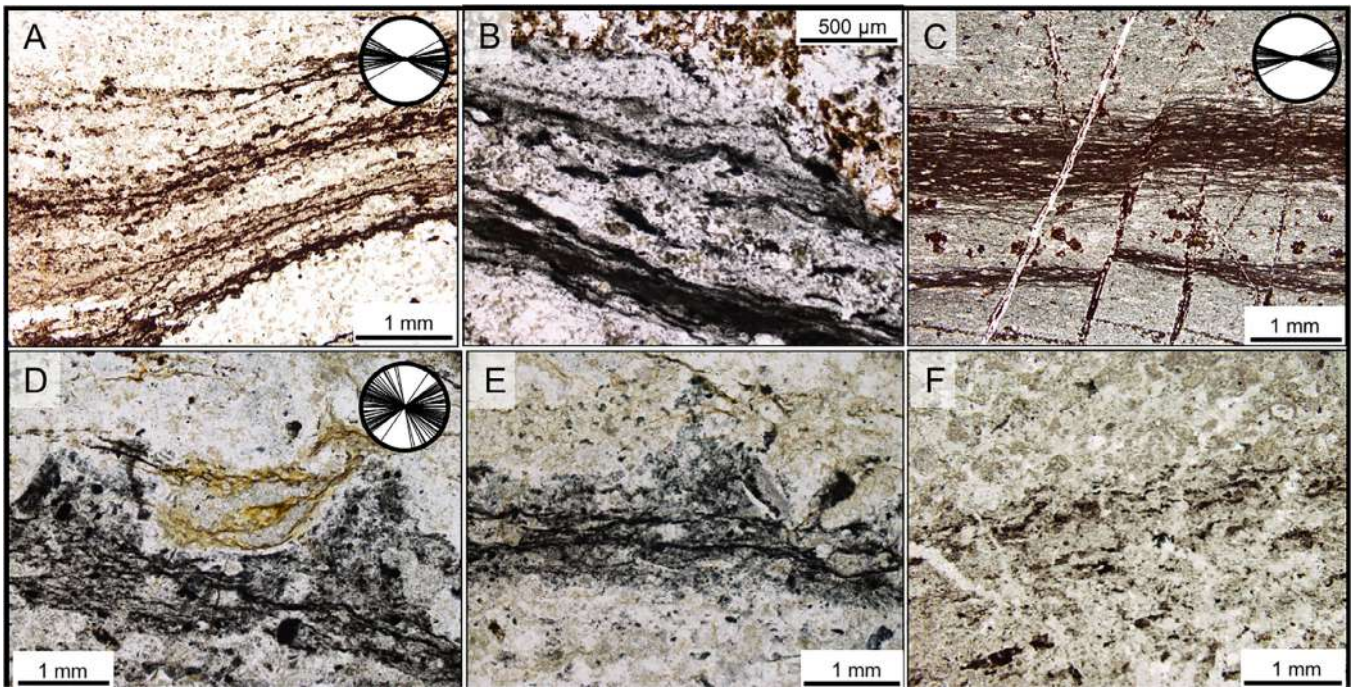

Fig. 9. Laminated textures from the Middle Marker horizon which are interpreted as of microbial genesis. Where applicable, a rose diagram of lamination or-ientations is provided; a dumb-bell shape is compatible with biological morphospace (after Noffke et al., 2013). (A and B) Crinkly, filament-like laminations, which have a gross structure of carbonaceous laminations intercalated with siliceous and volcaniclastic layers, and which mantle sedimentary textures of the host rock. (C) Low-relief, crinkly-wavy lamination, displaced by micro-faults. Note entrained quartz grains. (D and E) Pseudo-tufted carbonaceous laminations; rose diagram in D applies to both. (F) Degraded carbonaceous material in a laminated volcaniclastic sandstone, interpreted as being originally a pseudo-tufted lamination.

laminated carbonaceous sandstones and siltstones (Fig. 16A,C), the elevated I_{D1}/I_G ratio (1.11 1.46) and higher structural disorder ratio (52.5 59.3%) relative to massive clotted carbonaceous cherts (Fig. 16B; for which the same values are 1.05 and 51.3%, see Table 2) indicate a greater degree of structural disorder in the laminated facies. In contrast, the higher degree of structural order in the clotted carbonaceous chert together with the narrower D1 band suggest that it has undergone more severe thermal maturation (Marshall et al., 2007; van Zuilen et al., 2007). For Archaean samples, this thermal maturation is most parsimoniously linked to either metamorphism or localised hydrothermal alteration (Marshall et al., 2007; Sforna et al., 2014). Given the close proximity from which samples were collected, and the stratigraphic range over which they occur (the horizon is < 6 m thick) differential lateral or vertical metamorphism is an unlikely cause of the eventual differences in structural order, and thus the true reason must be both early diagenetic and local. By contrast, the laminated sandstones and siltstones contain stratiform silica veins, which are more consistent with a diffuse, distal hydrothermal scenario (after Hofmann and Bolhar, 2007; *cf*. Paris et al., 1985).

Dann and Grove (2007) note that the volcanic rocks beneath the Middle Marker are altered by seafloor hydrothermal processes, and this is unsurprising since every chert unit in the Barberton greenstone belt is underlain by such a diffuse, gradational hydrothermal sequence (Hofmann and Bolhar, 2007; Hofmann and Harris, 2008; Hofmann, 2011), as are si licified rocks in contemporaneous greenstone belts, e.g. the Nondweni (Hofmann and Wilson, 2007), and throughout the Warrawoona cherts of the Pilbara (Brasier et al., 2005, 2006). REE + Y data (MuQ normalised) for the samples studied herein exhibit trends which can broadly be de scribed as gradually increasing from LREEs to HREEs with positive Eu anomalies and occasional weakly positive Y anomalies (Fig. 5). This is indicative of the mixing of seawater with hydrothermal effluent (Bau and Dulski, 1996; Grassineau et al., 2002; Gourcerol et al., 2015, 2016). The sole REE + Y pattern with an inverse trend at high concentrations (04SA14; Fig. 5B), can be attributed to post diagenetic alteration (Gourcerol et al., 2015), and is therefore uninformative of the palaeoenvironment of its deposition. Extensive veins of percolating pure silica, which disrupt primary sedimentary structure and cause soft sediment deformation (Figs. 4D,F, 10A,B, 12E and 13A,B) further testify to the presence of some amount of contemporaneous hydrothermal fluid circulation during deposition of the Middle Marker, despite no recognition of these features by Lanier and Lowe (1982). An elevated silica content at the seafloor sediment interface, and thus early silicification, explains both the volumetric preservation of carbonaceous laminations (e.g. Fig. 12A,E) and the low degree of compaction throughout.

Considering the doubtless high concentration of silica in Precambrian oceans (Siever, 1992; Maliva et al., 2005; Knauth, 2005) and the necessity for high heat flux out of the interior of the ancient Earth (de Wit and Hart, 1993; Sleep et al., 2001; Ernst et al., 2016), the evidently early, syn depositional silicification of the Middle Marker rocks is probably most parsimoniously met by diffuse hydrothermal venting (Hofmann and Bolhar, 2007; Hofmann, 2011; Westall et al., 2018) into Si rich seas.

Our interpretation of the depositional environment of the Middle Marker is consequently a product of previous observations, *i.e.* shallow, wave active waters in the photic zone on a regionally extensive volcanically and hydrothermally active shelf.

6. Discussion II: Microbial palaeontology and assessments of biogenicity

6.1. Putative microbial features

A number of the carbonaceous features herein described can be considered microbially influenced (Fig. 9). The microstructures described in Section 4 are comparable to microbial mats, their erosional products, and their traces in the sedimentary record (microbially induced sedimentary structures such as biostabilization), as well as to proposed microfossils. These carbonaceous features can be broadly classified into four morphotypes:

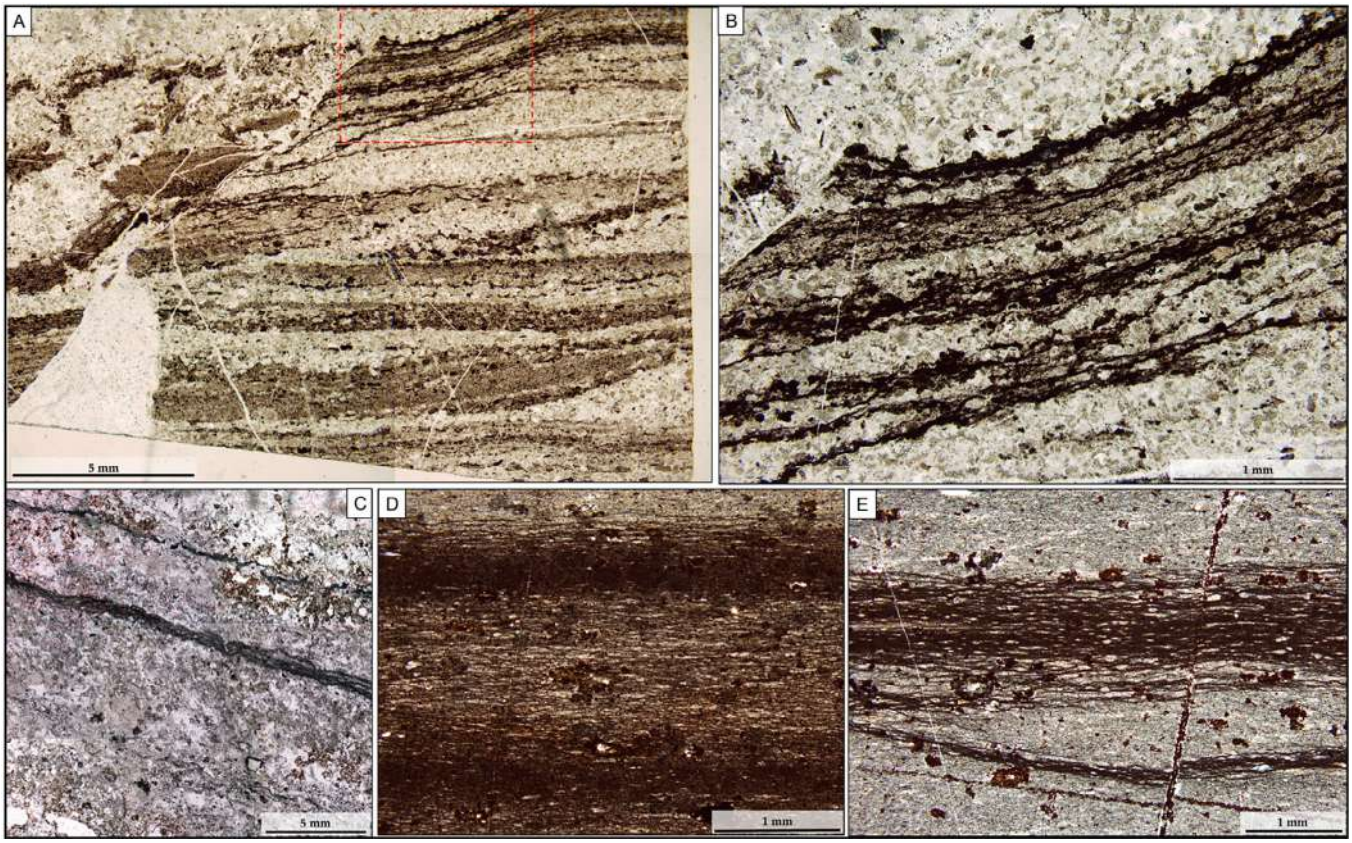

Fig. 10. Morphologies of crinkly, filament-like laminations interpreted as microbial mats. (A) Low-magnification view of multi-laminar microbial mats preserved over parallel and inclined stratification. Note the plastic deformation of carbonaceous laminations at the micro-fault (upper centre). (B) Higher-magnification image of the region outlined by the red box in (A). Laminations appear crinkly by virtue of their micro-tufted topography. Note the gross structure of carbonaceous laminae intercalated with lenses of silicified volcanic particles, and the thickening of carbonaceous laminae toward crests. (C) Low magnification photomicrograph of crinkly-wavy laminations in a coarse laminated volcaniclastic sandstone, occurring at the top of a graded sequence. (D and E) Low-relief, crinkly laminations which entrain oriented quartz grains. (D) has witnessed a greater degree of compression that (E). (E) exhibits plastic deformation. (For interpretation of the references to colour in this figure legend, the reader is referred to the web version of this article.)

i) fine, crinkly, biofilm like laminations;
ii) pseudo tufted laminations;
iii) wisps, flakes, and roll up structures;
iv) lenticular objects.

It is possible that some of these objects, namely wisps, flakes, and roll ups, are the erosional products of microbial mats (see Section 4.4.). Additionally, where no cellular organic matter is preserved, a combination of i) morphospace, ii) indications of *in vivo* cohesiveness re sulting from sediments being bound by glutinous EPS (Decho, 1990; Sutherland, 2001; Neu et al., 2003; Gerdes et al., 2000), and iii) lamina grain interactions (see Section 4.3) can shed light on initial biogenicity. Such traces are termed microbially induced sedimentary structures (MISS, *cf.* Noffke et al., 2001). Laterally differential taphonomy of pu tative microbial fabrics in the Middle Marker occasionally results in no carbonaceous material being preserved (Figs. 4A and 15D).

The volumetric significance of putative microbial fabrics is relatively minor: they occur as thin, regular, horizons of < 200 μm to ~ 2500 μm thickness dependent upon morphotype. Multiple morphotypes of laminations can occur within a single sample, though fine, crinkly, film like laminations (Figs. 10 12) are the most common. One axiomatic trend is that putative microbial horizons are anticorrelated with the deposition of volcaniclastic material, occurring always at the apogee of graded sequences, during the erosional regime. This is entirely consistent with the occurrence of mat fabrics described by Noffke (2003, 2010) and Tice (2009). From the sedimentological model advanced by Lanier and Lowe (1982), this suggests that they developed mostly during pauses between magmatic pulses during the waning volcanic cycle. Indeed, our sedimentological interpretation corroborates that of Lanier and Lowe (1982), with the addition of diffuse hydrothermal activity to account for (i) near pure silica layers; (ii) perco lating veins of silica which occurred syn depositionally and disrupted sedimentary fabric; and (iii) exceptional volume preservation of putative microbial fabrics. The presence of hydrothermal activity is unsurprising, presumably originating from the ubiquitous volcanic systems which characterised the Early Archaean surface environment (Sleep et al., 2001; Brasier et al., 2005, 2006, 2013; Van Kranendonk, 2006, 2007; Westall et al., 2011, 2015; Arndt and Nisbet, 2012; Westall, 2016).

The abiotic null hypothesis (*cf.* Brasier et al., 2004) to be overcome in the case of all putative microbial features is "that laminated features reflect sedimentary horizons, pressure solution fronts, or diagenetic mineralisation, and that taphonomic differences are purely the product of differential primary sedimentation".

6.2. Assessment of biogenicity

Thorough assessments of biogenicity are requisite in the proof of all ancient biosignatures (Buick, 1990; Brasier et al., 2005; Wacey, 2009; Westall and Cavalazzi, 2011) and an assertion of biology is worthless without proof of (i) occurrence in an environment clement to life; (ii) syngenicity of the object of interest with the primary rock fabric; and (iii) objectivistic, non reductive assessments of biogenicity against a wide range of criteria. This culminates in an argument for biogenicity which, since the Archaean geological record preserves an imperfect fossil record, obeys classical rationalism in its reason and deduction.

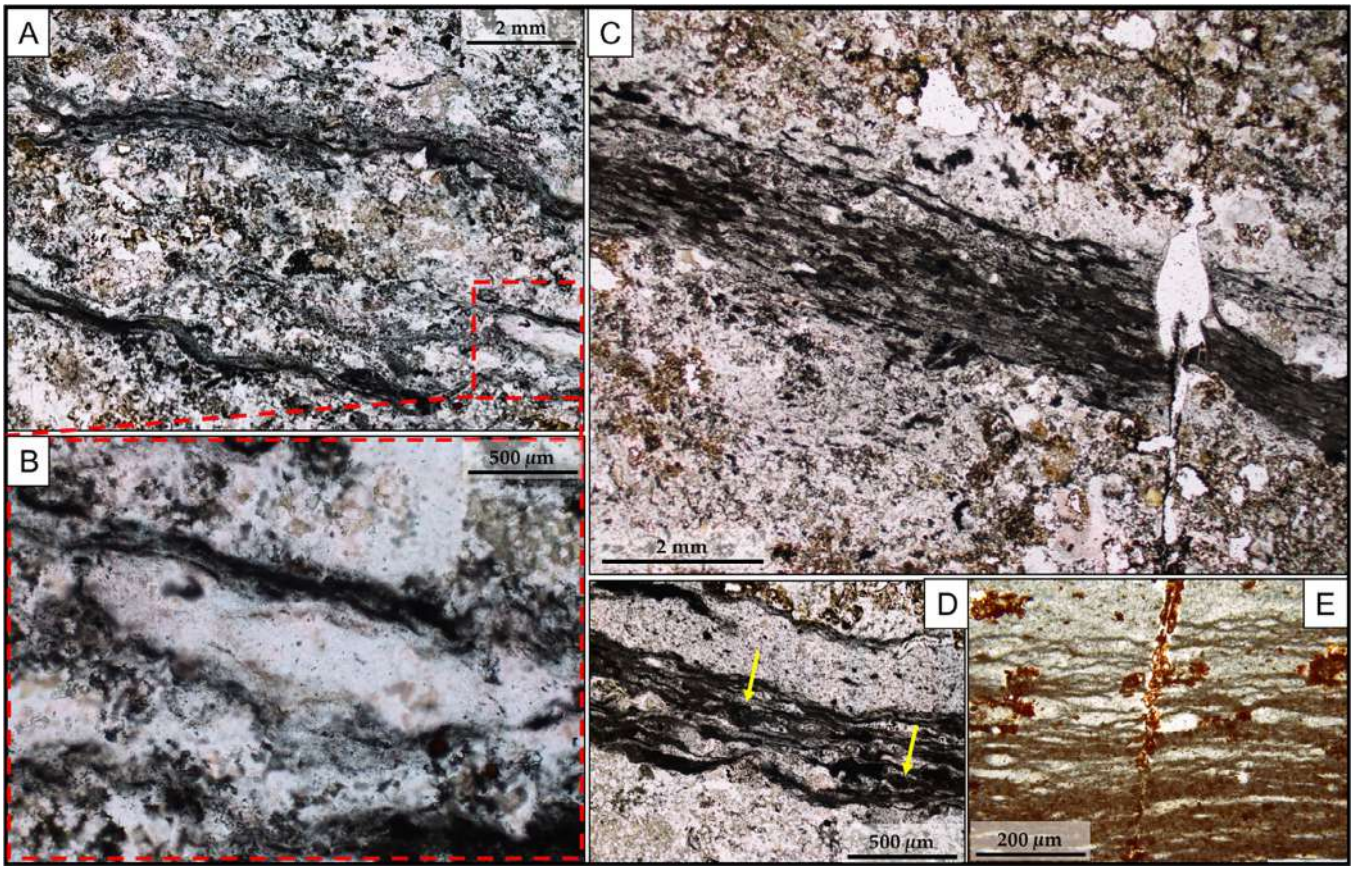

Fig. 11. Characteristic features and details of crinkly, filament-like microbial laminations interpreted as microbial mats. (A) Multi-laminar microbial mat which surrounds a mass of pyroclastic, volcaniclastic material. Structure in (B) is indicated by red box. (B) Individual laminae surround a silica lense. (C) Crinkly-wavy laminations in a coarse laminated volcaniclastic sandstone, overlain by coarse pyroclastic material which inhibits microbial growth. Note the mantling of the rhombic grain below (lower centre). (D) Crinkly laminations within which are lenticular objects (arrowed). See Fig. 16 for further examples and Section 4.4. for detailed explanation. (E) Trapped, baffled, oriented quartz particles within an interpreted microbial mat. (For interpretation of the references to colour in this figure legend, the reader is referred to the web version of this article.)

6.2.1. Geological plausibility

The Middle Marker sediments represent a shallow marine environment associated with volcanic activity (Lanier and Lowe, 1982) in the vicinity of minor hydrothermal outflow, a situation entirely compatible with the environmental settings of Palaeoarchaean marine microbial consortia from throughout the Kaapvaal and Pilbara cratons (e.g. Walter et al., 1980; Schopf and Walter, 1983; Buick, 1984; Walsh, 1992; Westall et al., 2001, 2006, 2011, 2015; Noffke et al., 2003, 2006a,b, 2013; Sugitani et al., 2007, 2010; Hickman Lewis et al., 2016; Oehler et al., 2017). Modern microbial mat communities readily occur in si milar tidal intertidal settings (Gerdes and Krumbein, 1987; Gerdes, 2007; Noffke, 2003, 2010). The Middle Marker would thus have been a promising niche for the flourishing of phototrophic and, presumably, symbiotic chemotrophic communities on a large spatial scale, being a moderately thermophilic, photic zone setting. It seems to have been within the stream of metal fluxes from volcanic (Fig. 5A) and hydro thermal sources (Fig. 5B) and in an environment where currents would create a nutrient flux. This is consistent with Early Archaean microbial biomes (Nisbet and Fowler, 1996; Nisbet, 2000; Nisbet and Sleep, 2001; Grosch and Hazen, 2015).

Prokaryotic microbial communities appear to have endured on the Earth for at least 3.5 Ga (Altermann and Kazmierczak, 2003; Schopf, 2006; Wacey, 2009; Westall and Cavalazzi, 2011; Hickman Lewis et al., ac cepted), and thus these ecologies are entirely compatible with both the age and environment of the formation. Since the Middle Marker appears not to have undergone early catagenesis or metamorphism (Delarue et al., 2016), high fidelity primary preservation is expected and recognised.

6.2.2. Textural syngenicity

All interpreted microbial mat horizons are conformable with bedding or cross stratification in the Middle Marker sediments and are constant across individual thin sections and hand samples (Figs. 9 13 and 15). Putative microbial fabrics always occur at the top of graded volcaniclastic layers, *i.e.*, they exhibit preferential growth at specific surfaces. Such similarity indicates a pattern of episodic growth of putative microbial laminations governed by clastic and marine inputs to their environments. Putative microbial fabrics in the Middle Marker are endemic to laminated volcaniclastic sandstones and siltstones, although a restricted range of fabrics are detected in coarse grained volcani clastic sandstones. Differential preservation potential may influence this distribution.

Most laminations drape and enwrap adjacent grains: this trapping baffling behaviour is often described in chemotrophic and phototrophic microbial sediments and necessarily occurs during formation (Oschmann, 2000; Noffke, 2010; Noffke et al., 2003, 2006b, 2013; Homann et al., 2015). The syngenicity of putative microbial features with their host rocks is thus incontestable.

All proposed microbial morphologies have undergone similar degrees of lower greenschist metamorphism, and have broadly similar thermal maturities, as indicated by Raman spectra in Fig. 16 (Dziggel et al., 2002, 2006; van Zuilen et al., 2007). Raman spectral analyses from points within the microstratigraphy of a pseudo tufted lamination show no trend, and thus indicate no differences in maturity throughout: this, and other, microbial fabrics are thus texturally syngenetic and exhibit responsive growth to their sedimentary environment. The eventual shared granular taphonomy of all carbonaceous microbial like

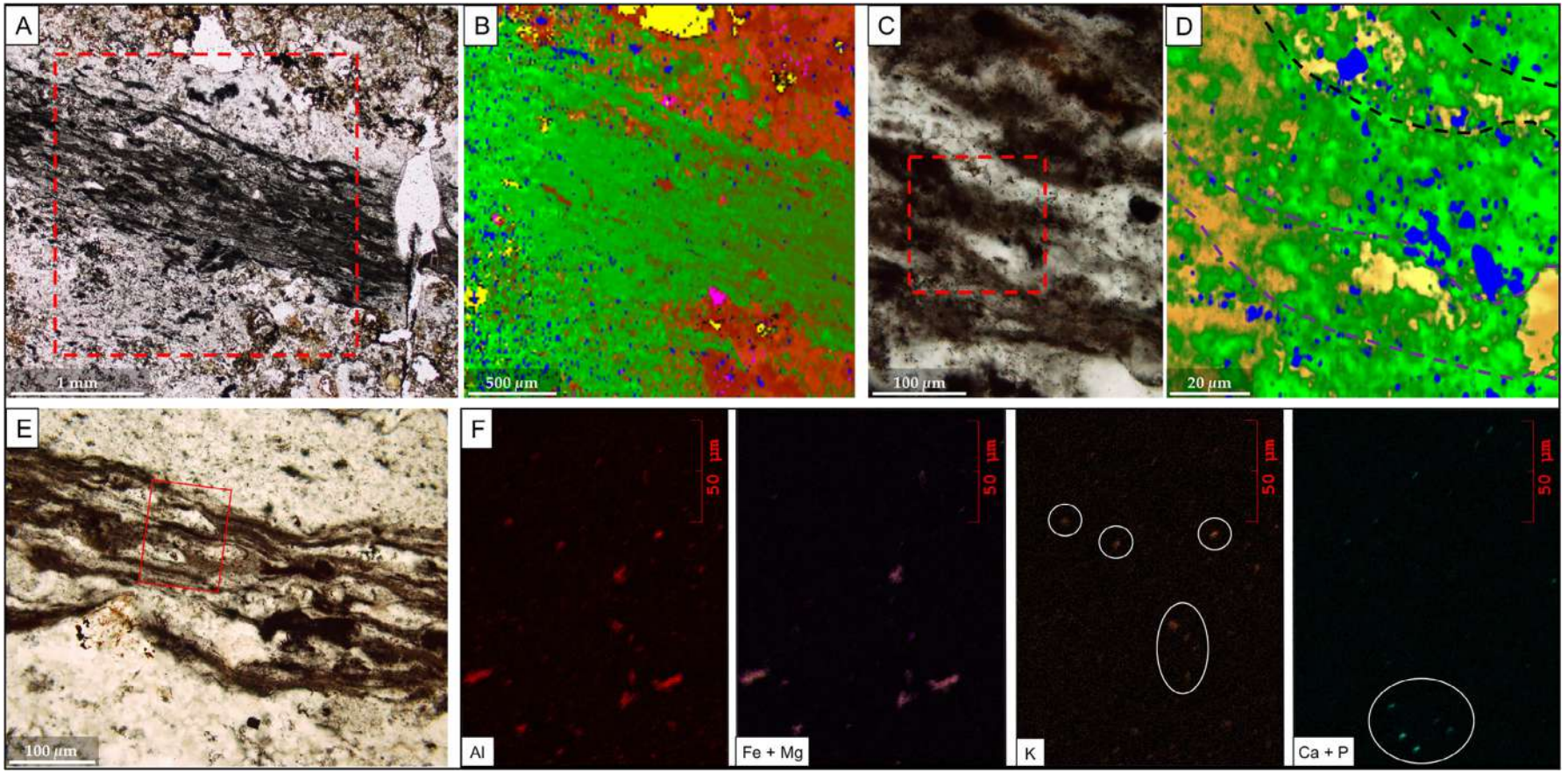

Fig. 12. Raman and SEM-EDX mineralogical and elemental mapping of carbonaceous crinkly, filament-like laminations in laminated volcaniclastic sandstones-siltstones, interpreted as microbial mats. (A) Photomicrograph of thick lamination; red box indicates area of Raman mineralogical map in B). B) Raman spectroscopic map, in which carbonaceous material = green, quartz = orange, anatase = blue, siderite = pink, araldite (resin) in voids = yellow. Note the concentration of carbonaceous material both within the microbial mat and within the clotted fabric directly below. A gross structure of carbonaceous material separated by volumetrically inferior siliceous lenses oriented parallel to the laminae is clear. (C) High-magnification image of the crinkly, filament-like lamination. Red box indicates area of Raman mineralogical map in (D). (D) Raman spectroscopic map in which carbonaceous material = green, quartz = yellow-orange and anatase = blue. Dotted lines indicate the gross structure, and separate lamina regions (dominated by carbon) and lense regions (dominated by quartz). (E) Crinkly-wavy lamination. Red box indicates the region mapped by SEM-EDX in (F). (F) SEM maps of Al, Fe + Mg, K and Ca + P, demonstrating that, in addition to quartz, oriented particles of both mafic and felsic volcanogenic material have been trapped within the mat. The map of K likely indicates unsilicified feldspathic grains, and Ca + P indicates apatite grains. (For interpretation of the references to colour in this figure legend, the reader is referred to the web version of this article.)

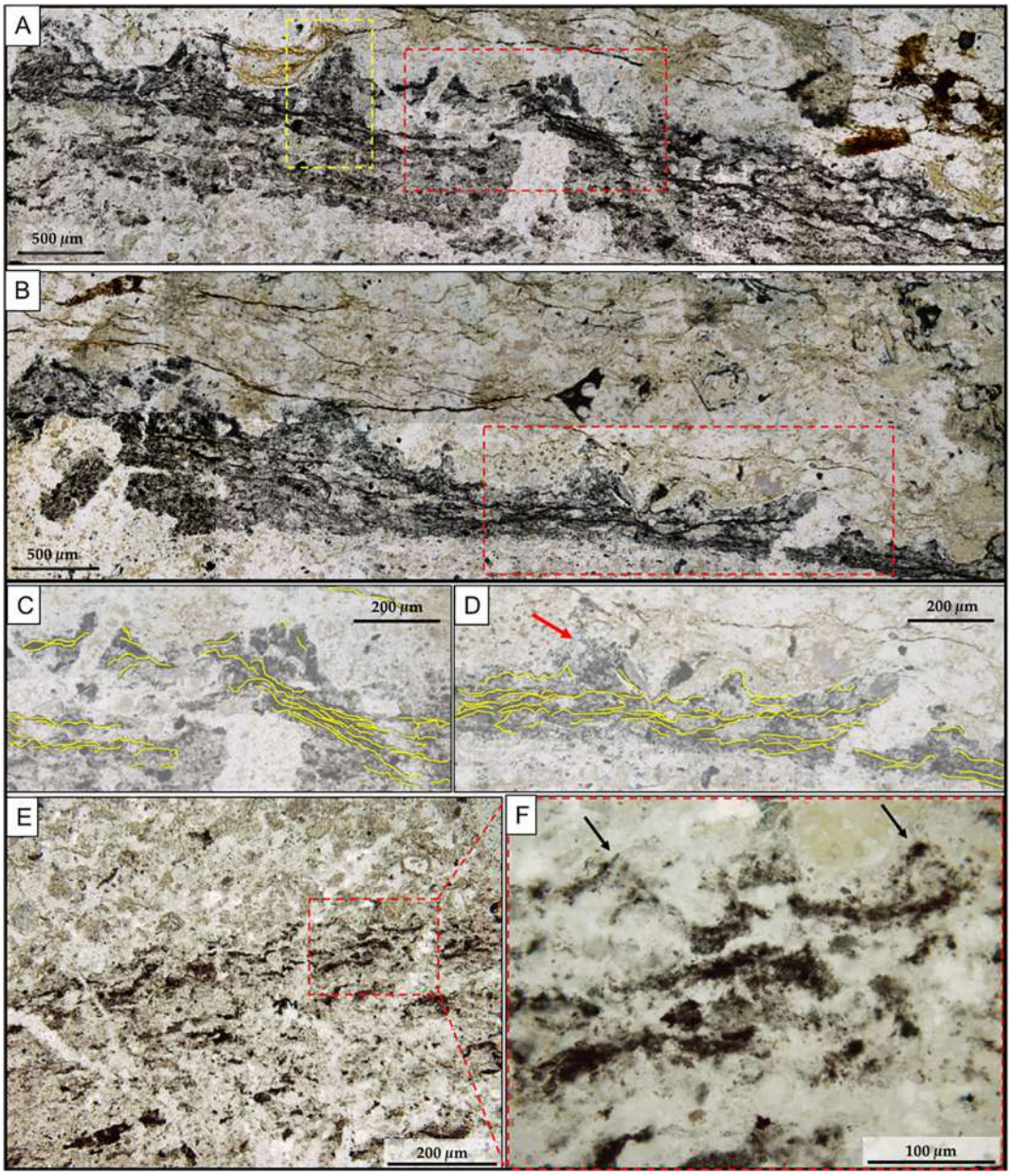

Fig. 13. (A and B) Tufted layers in laminated volcaniclastic sandstones and siltstones, interpreted as pseudo-tufted microbial mats. These are dark grey, carbonaceous edifices with clear peaks and troughs which represent a secondary morphology (see main text for explanation). Crinkly, biofilm-like laminations are common in the lower part of the layers, and occasionally reach the crests. Red box in A indicates the region shown in C; red box in B indicates the region shown in D; yellow box indicates the region of the Raman spectroscopic mapping in Fig. 13. (C and D) Interpretation of the occurrence of individual crinkly biofilm-like laminae within mats. Note that across both tufts, there is small amount of preservation of biofilm within the crest region, suggesting that tufts are coeval with the laminae below. In the tuft, granular fabrics dominate, which may have formed due to Ostwald ripening of silica spherules (red arrow). (E and F) Carbonaceous layers with a weakly preserved tuft-like morphology, interpreted as degraded pseudo-tufted microbial mats. Red box in E indicates region of F. Arrows in F indicate probable ex-tufts. There is little to no preservation of interpreted microbial biofilms therein. (For interpretation of the references to colour in this figure legend, the reader is referred to the web version of this article.)

features in the Middle Marker argues strongly against a sedimentolo gical origin, for which a continuum of eventual 'taphonomies' would be expected. Thus, the likelihood of these morphologically diverse laminations having an identical sedimentary precursor is highly improbable. This refutes the null hypothesis asserted in Section 6.1, and further supports the biological interpretation.

6.2.3. Biogenicity

In the following sections, we assess the biogenicity of the five morphotypes of microbial like features through comparison of shared traits with similar structures, and through testing against a range of biogenicity criteria.

i) Fine, crinkly, laminations

Fine, crinkly laminations are superficially similar to thin fossil microbial biofilms. Their stratigraphic context, occurring always at sedimentary inflection points in shallow water marine deposits between volcanic eruptions, is consistent with the occurrence of proposed biofabrics in cherts of the Mozaan Group (Noffke et al., 2003), Hooggenoeg Formation (Walsh and Lowe, 1985, 1999; Walsh, 1992; Walsh and Westall, 2003; Tice and Lowe, 2004; Tice, 2009), Josefsdal Chert (Westall et al., 2006, 2015), stratiform Apex chert (Hickman Lewis et al., 2016, 2017) and Dresser Formation (Noffke et al., 2013). There is a particularly close morphological resemblance between these laminations and those of the contemporaneous Dresser Formation and younger

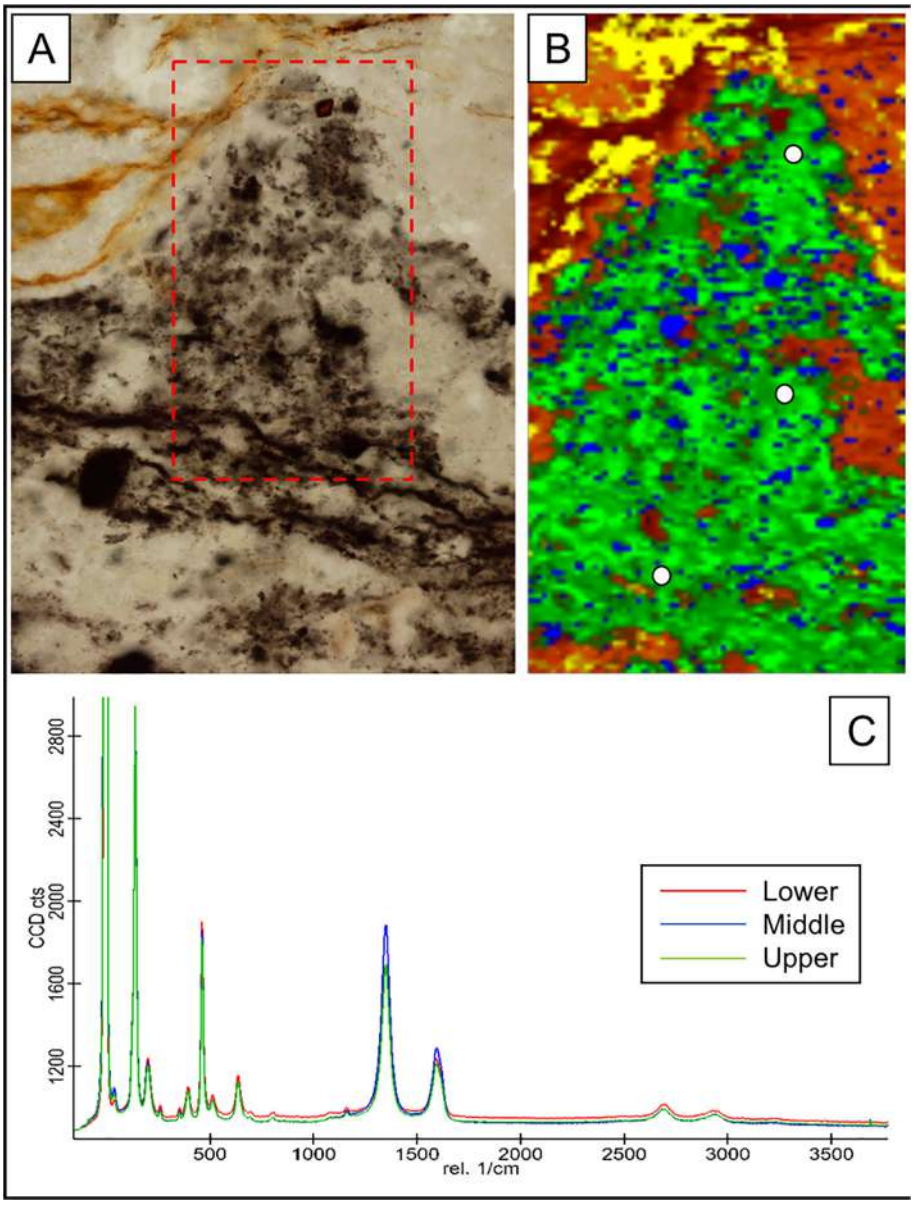

Fig. 14. Raman spectroscopic mapping and point analyses within the tuft indicated in Fig. 12A. (A) Photomicrograph in plane-polarised light of single tuft, with laminated base and granular crest. Red box indicates region of B. (B) Raman spectroscopic map, in which carbonaceous matter = green, silica = orange, anatase = blue, and araldite (resin) = yellow. The three white circles indicate the point spectra displayed in (C). (C) Point spectra of carbonaceous material in the lower mat-like region, and middle-upper granular regions. Indistinguishable spectra suggest syngenetic carbonaceous material. (For interpretation of the references to colour in this figure legend, the reader is referred to the web version of this article.)

Mozaan Group, both of which have been classified as microbial mats or microbially induced sedimentary structures.

Individual laminae are non isopachous and exhibit anastomosis in compatible with a sedimentary or diagenetic precursor. In most cases, plastic deformation cannot be attributed to compaction or particle settling, and thus the varying thickness of the layers is primary (Figs. 10 12). This primary, non isopachous character has been erected as a biogenicity criterion for microbial mats growing in the presence of sunlight (Buick, 1984; Pope and Grotzinger, 2000; Pope et al., 2000).

These putative microbial biofilms meet most of the morphological criteria for biogenicity:(i) they are fine, kerogenous laminations which alternate with pure silica layers and lenses, each lamination being 5 30 μm thick and slightly wavy, with a crinkled relief of no more than 0.5 1 cm (Walsh, 1992; Walsh and Westall, 2003; Gerdes, 2007; Noffke et al., 2013); (ii) they are wavy or crinkly on both large and small spatial scales (compare Figs. 10B and 11C), and are laterally dis continuous at the micron scale, but broadly continuous at the centi metre scale (Walsh and Lowe, 1999; Walsh and Westall, 2003; Greco et al., in review); (iii) their gross structure approximates that of modern microbial mats, *i.e.* they alternate layers of organic rich material with a film or filament like construction (*cf*. Hickman Lewis et al., 2017) with layers of detrital material or entrained particles (Figs. 10B, 11 and 12C,D; Noffke et al., 2001; Noffke, 2009, 2010); (iv) the presence of folded, torn, crumpled and rolled fragments demonstrably indigenous to the laminations strongly implies an initial cohesive plasticity (after Simonson et al., 1993; Sumner, 1997; Walsh and Westall, 2003; Tice and Lowe, 2004); (v) their non isopachous laminae thicken toward crests (Figs. 10A,B and 11; Pope and Grotzinger, 2000; Pope et al., 2000), suggesting growth out of the laminar bottom flow waters toward more dynamic, nutrient rich waters above (Gerdes, 2007); (vi) they mantle macro scale features such as bedding planes, cross stratification (Fig. 10A,B) and sediment lenses (Homann et al., 2015); and (vii) their growth is templated by the underlying grain topography and entrained particles are oriented (Fig. 11), suggesting an effort to bio stabilise the sedimentary surface during colonisation (Gerdes et al., 1991; Noffke, 2003; Noffke et al., 2003, 2013; Heubeck, 2009; Gerdes, 2007). These seven lines of evidence convincingly demonstrate that these structures were surface colonising, biostabilising biofilms. Their micro tufted and crinkled relief resembles that of anoxygenic, photosynthesising microbial communities (Tice and Lowe, 2006; Heubeck, 2009). Intimate intergrowth with bound substrate grains suggests originally glutinous, mucilaginous material *i.e.* extracellular polymeric substances (EPS; Noffke, 2003; Westall et al., 2006). The original filamentous texture may have been 'hazed' by diagenetic processes ("*Archaeanisation*"; after

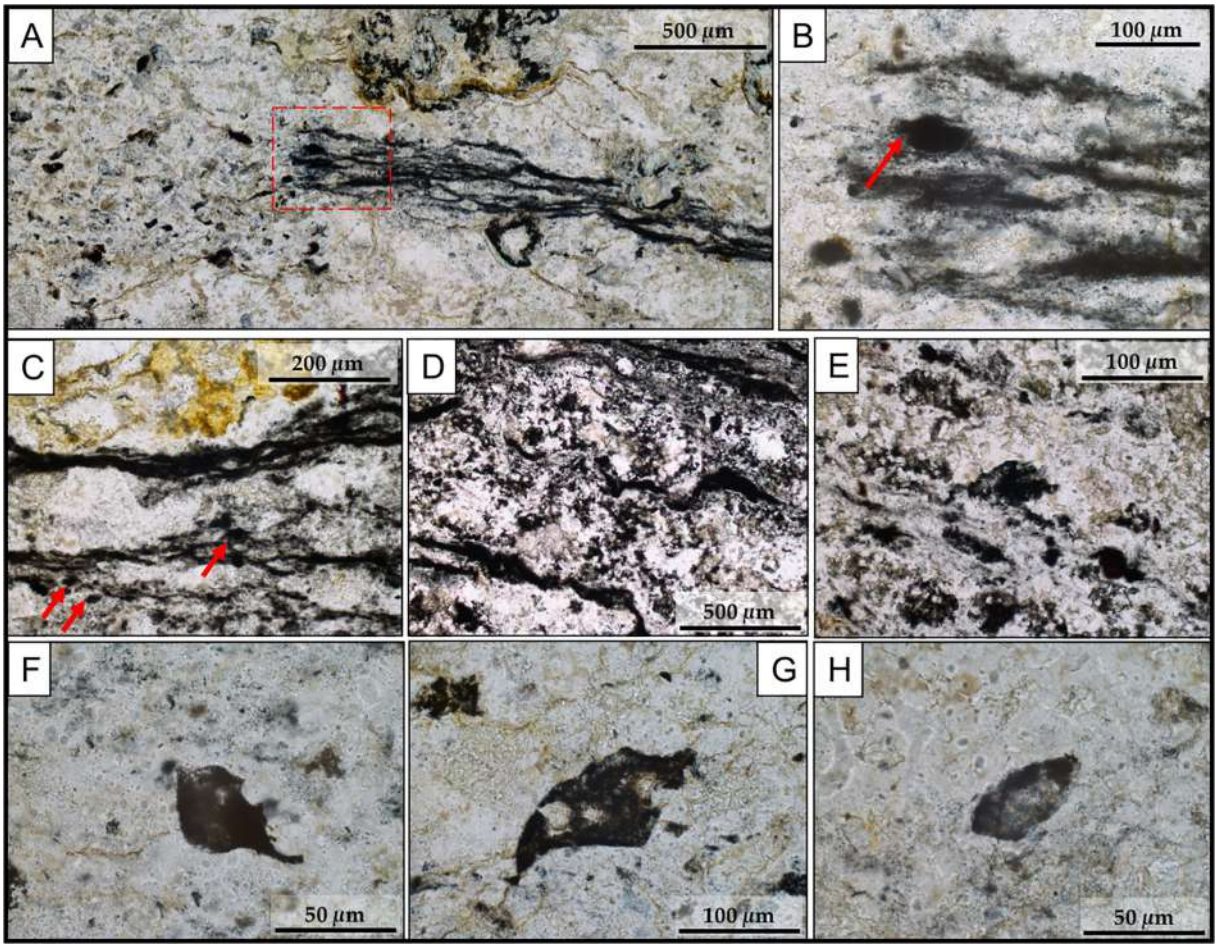

Fig. 15. Associations of wisps, flakes and lenticular objects with crinkly, filament-like microbial mats. (A) Frayed mat in a laminated volcaniclastic siltstone, with randomly distributed carbonaceous detritus, including flakes and lenticular objects, in the adjacent matrix. Red box indicates region of (B). (B) High-magnification view of the region outlined in A, showing a lenticular object (arrowed), which is clearly contiguous with the primary lamination of the mat fabric. (C) Lenticular objects occurring as part of the primary lamination of another crinkly, filament-like microbial mat. (D) Non-isopachous, elongate wisps or flakes in the matrix between two microbial mats. The base of one such mat is visible to the upper right. (E and H) Lenticular objects of differing composition, found randomly oriented in the matrix of mat-rich, volcaniclastic siltstones. E and F are carbonaceous, G is an altered volcanic particle, H is anatase. (For interpretation of the references to colour in this figure legend, the reader is referred to the web version of this article.)

Knoll et al., 1988; Noffke et al., 2006b), accounting for the lack of individual architect microfossil aggregations preserved within the mats.

The micro tufted relief is of near identical dimensions to tufted crinkle microbial laminations in the contemporaneous Dresser Formation (Noffke et al., 2013), which are interpreted as indicators of growth in the subtidal zone (Gerdes and Krumbein, 1987; Noffke et al., 2001). Their multi laminar morphology signifies continuous and successful growth during the transient habitable niche between volcanic inputs; indeed, in modern microbial mats a microbial biofilm may begin to colonise a surface in only tens of minutes (Paterson et al., 1998, 2003; Busscher and Mei, 2000). Laterally discontinuous crinkly biofilm 'fragments' may suggest growth in a stressed environment, in which the struggle to grow was balanced against resilience to volcaniclastic input. Based on assertions of such morphologies being indicative of phototrophic metabolisms (e.g. Bosak et al., 2009; Flannery and Walter, 2011), the crinkly, finely laminated biofilms of the Middle Marker are interpreted as the remains of areally extensive, probably anoxygenic, photosynthetic communities flourishing in water depths of not more than 5 10 m (after Noffke et al., 2006a; Homann et al., 2015).

ii) Pseudo tufted laminations

Pseudo tufted laminations bear considerable resemblance to modern and ancient microstromatoloid like structures (Gerdes, 2007; Homann et al., 2015), the fossil examples of which are often interpreted to indicate photosynthesis (Bosak et al., 2009, 2013; Flannery and Walter, 2011; Gamper et al., 2012). Interpretive diagrams illustrating the trajectories of laminae within tufted horizons show that some, but not all, laminations appear to continue upward into the crests (Fig. 13C,D). However, many troughs between tufts are associated with the settling of dense particles from the water column, thus soft sediment deformation is a likely cause of this topography, in contrast to the unambiguously primary micro tufted topography of fine, crinkly microbial mats.

The fine, crinkly laminations bear morphological similarity to both the fine, crinkly laminae described above and *alpha type laminations* from the 3.42 Ga Buck Reef Chert, interpreted as microbial mats by Tice and Lowe (2006) and Tice (2009). Although the Middle Marker laminations are less well preserved, several salient similarities are noted: (i) they anastomose and bifurcate around carbonaceous particles and can form lamina stacks (Fig. 13A D and 14A); (ii) they have near-constant, slightly variable lamina thickness; (iii) they crumple and fold (Fig. 13C,D), indicating cohesive strength at the sediment surface (Neu et al., 2003) during deposition and diagenesis; and (iv) they occur in a microfacies which is rich in simple carbonaceous grains, mat like laminations and silicified grains, but poor in terrigenous detrital matter (*cf.* microfacies III of Tice and Lowe, 2006). These four lines of evidence strongly support a biogenic interpretation. The sub millimetric relief of laminae, together with a crinkly, wavy laminar morphology, are evocative of photosynthetic microbial mats (Gerdes, 2007;

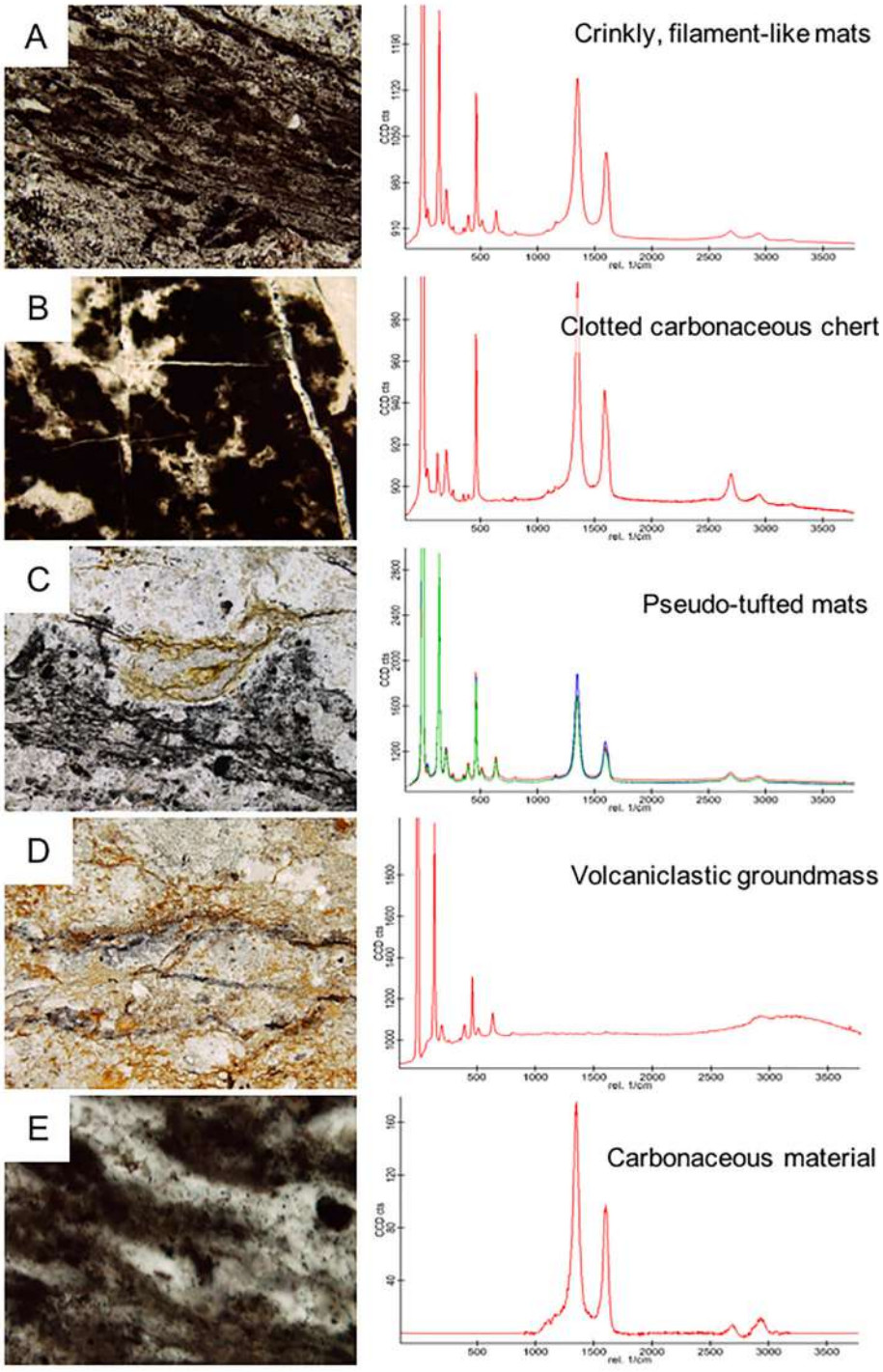

Fig. 16. Comparison of Raman spectra between different occurrences of carbonaceous matter in the Middle Marker. (A) Spectrum from laminae incrinkly, filament-like microbial mats. (B) Spectrum from clots in massive, clotted carbonaceous cherts. (C) Spectrum from laminae and microclasts in tufted microbial mats. (D) Spectrum from volcaniclastic groundmass for comparison; note the dominance of the anatase signal. (E) Extracted signal from carbonaceous material from crinkly, filament-like laminations, which constitute the most promising biosignature in the Middle Marker. See Table 2 for spectral analyses.

Table 2
Raman spectral parameters.

Structure	I_{D1}/I_G	$I_{D1}/(I_{D1} + I_G)$
Fine, crinkly, biofilm-like lamination	1.11	52.6
Pseudo-tufted lamination	1.28–1.46	57.8–59.3
Clotted carbonaceous material	1.05	51.3

Heubeck, 2009; Bosak et al., 2009), thus these likely represent epibenthic, probably anoxygenic, photosynthetic communities.

Speculatively, it is possible that a stratified microbial community is present in the lower and middle upper regions: the microbial mats directly overlie clotted carbonaceous textures, which have been interpreted as biomass clumps (Walsh and Lowe, 1999) and as degraded chemotrophic colonies (Westall et al., 2015). A similar interstratified relationship between mats and clots exists in Hooggenoeg cherts (Walsh, 1992; K. Hickman Lewis, unpublished data) and in the Jo sefsdal Chert (Westall et al., 2015). Autotrophic heterotrophic

symbiosis results long term stability of the overall system (Decho and Kawaguchi, 2003), and such community structure maximises the ecological efficiency of biomass (Reitner, 2010), indeed, microbial stratification occurs naturally as a result of micrometre scale gradients in microbial mats (Revsbech, 1989).

iii) Wisps and roll up structures

Isolated wisps are elongate, tapered carbonaceous objects which float in the silica matrix. Interpretations of their origins include (i) compressed products of lobate carbonaceous particles (Walsh and Lowe, 1999), (ii) eroded and redeposited fragments of shale grade, clay rich sediment (Schieber et al., 2012); (iii) ripped up fragments of microbial mat (Schieber, 1986, 1998; Schieber et al., 2007, Noffke, 2010) or natural biofilm detachment (Busscher and Mei, 2000; Neu et al., 2003), and (iv) ambiguous objects of equally probable biological or sedimentary origin in the absence of identification of the parent structure (Hickman Lewis et al., 2016).

It is difficult to trace the protolith of wisp or flake like structures in Archaean rocks, thus biological inferences are made on dimensional comparisons with known microbial mats. Where dimensions are roughly equivalent, and where morphology suggests initial plasticity (Schieber, 1986, 1998), a biological origin may be reasonably supposed. This is true for the wisps and flakes described in the Middle Marker cherts. Their compositional and dimensional similarity to fine, crinkly microbial mats, and their occurrence in the vicinity of fractured mats, suggest that wisps and flakes represent the eroded fragments of microbial mats. Preserved tear up structures at the surfaces of crinkly mats evidence their erosion *in situ*.

iv) Spindles and lentils

In the first systematic description of Archaean microfossils, Walsh (1992) designated spindle like carbonaceous microstructures in Hoog genoeg and Kromberg cherts to be probable fossils since they passed six of the seven criteria for biogenicity set down by Buick (1990). Since that study, the range of described spindle like and lenticular objects has proliferated, and their interpretation as microfossils is now presumed (Sugitani et al., 2007, 2009, 2010, 2015; Grey and Sugitani, 2009; Oehler et al., 2009, 2017; House et al., 2013). Walsh (1992) deemed that the central cavity in most spindles precluded their identification as carbon coated gypsum crystals, and independent mineralogical identifications confirm that they are often carbonaceous and can contain organic contents inter preted as degraded cellular remains (Sugitani et al., 2010, 2015). Their size distributions (Walsh, 1992; Sugitani et al., 2009) usually support a biolo gical, rather than mineralogical, identity.

Lenticular objects in the Middle Marker are found within fine, crinkly microbial mats (Fig. 15). The objects we identify bear con siderable morphological similarity to those of past studies, though are of great compositional variation, from vitreous, glassy material (phyl losilicates; Fig. 15D) to carbon (Fig. 15E,F). Additionally, their occur rence as seemingly entrained particles in interpreted microbial mats (Fig. 15B,C), and their dispersion into the microcrystalline matrix with other eroded mat fragments mean that it is impossible to distinguish them from other detrital entrained objects. There is no indication of their being part of the mat building community, nor do they exhibit the community like behaviour shown by other lenticular microfossil like objects (e.g. Sugitani et al., 2015).

Walsh (1992) noted that by comparison to recent microfossils, poor preservation had rendered the morphology of spindle or lentil like microfossils too simple to draw parallels. The lenticular objects described herein pose a similar challenge. Although a large amount of data exists to support the biogenicity of other occurrences of lenticular microfossil like objects, our own findings, together with observations by others (D. Wacey, personal communication), support that some of these objects are simply grains of detrital entrained volcanogenic material within microbial mats. Therefore, we find no evidence for a biological interpretation of lenticular objects in the Middle Marker horizon.

6.2.4. Cautions and considerations in the biological interpretation 6.2.4.1. Size range. Although carbonaceous laminations in Early Archaean cherts are frequently interpreted biologically, several shortcomings persist in this assertion, apart from the degradation of their organic material through diagenesis and taphonomy.

Archaean phototrophic biofilms are much less thick than the modern examples with which they are equated, comprising sets of la minae which are usually less than tens of microns in thickness, and having total thicknesses of less than several hundred microns (Golubic, 1976; Monty, 1976; Margulis et al., 1983). This issue can be cir cumnavigated *via* two explanations.

Walsh (1992) and Walsh and Lowe (1999) suggest that compaction during diagenesis may cause this thinning. Westall et al. (2006, 2015) have implied that it could be the result of anaerobic biomass having low growth rates; indeed, it is known that anoxygenic microbes produce biomass at a rate much slower than oxygenic organisms (McCollum and Amend, 2005; Parkes et al., 2014). Comparing these possibilities, a fundamental me chanical dichotomy exists in the compaction hypothesis: since both carbo naceous particles and flattened wisps occur at the same millimetric strati graphic level, yet the former are sometimes judged to produce the latter (Walsh and Lowe, 1999), it is irreconcilable that both can exist in concert. This is evident even in photomicrographs from Walsh and Lowe (1999). Considering the metabolic hypothesis, the disparities in both biofilm size and thickness of biofilm packets are minimised if one considers chemo synthetic microbial mats composed of either modern (Bailey et al., 2009) or fossil (Cavalazzi, 2007; Cavalazzi et al., 2007; Homann et al., 2016) fila mentous microbiota. Thus, the second hypothesis is most plausible. Con sequently, this study finds no untenable smallness in the size exhibited by putative microbial mats that could preclude a biological interpretation.

6.2.4.2. Metabolism. Since chemotrophic microbes can only be definitively delineated from phototrophic microbes by gene sequencing analyses of the architect community (Williams and Reimers, 1982), and since the preservation of interpreted microbial mats in the Middle Marker is of insufficient fidelity to identify individual fossils, it is impossible to estimate the relative roles played by chemosynthetic and photosynthetic metabolisms. However, it is known that the Archaean Earth was largely anoxic, and thus widespread mats such as these should not be expected to have performed oxygenic metabolism, a standpoint supported by phylogenetics (Batustuzzi et al., 2004). Walsh (1992) highlights that, through geological time, phototrophs have tended to dominate the shallow water niche. Specific topographic morphologies, such as tufts, also have a strong affinity to phototrophic microbes (Bosak et al., 2009). For these reasons, it is supposed that the microbial fabrics described herein were built by anoxygenic phototrophs.

6.2.4.3. Alternative, abiotic formation of wisps and flakes. As explained above, for wisps and flakes, the erosion of fine grained, clay rich, carbonaceous sediment has been experimentally demonstrated, using flume equipments, to produce flake rich sediment of entirely abiotic genesis (Schieber et al., 2012). Thus, despite inferring the erosion of microbial mats in the formation of wisps and flakes, it is impossible, at this time, to prove this without knowing the exact provenance of the organic material. Nonetheless, the explanation in Section 6.2.3. provides support for the biogenicity of wisps and flakes.

6.2.4.4. The conundrum of lenticular objects. In Middle Marker metasediments, lenticular objects occur as entrained particles within the laminae of interpreted microbial mats, and as isolated, seemingly eroded objects from these mats (Fig. 15). Their wide range in size, their highly variable composition and mineralogy, and their striking resemblance to natural variations in laminar thickness within the mats argue for variable, abiotic mechanisms of formation.

7. Discussion III: The Middle Marker horizon and its microbial inhabitants as the oldest example of a globally important, Early Archaean biocoenosis

Presented herein is a document of the oldest fully developed microbial ecosystem inhabiting a particular marine environment that appears to have been common in the Early Archaean of the Barberton greenstone belt, and seemingly also in the Pilbara. The evolution of the Middle Marker horizon is synthesised in Fig. 17. Together with evidence from other Early Archaean habitats, major trends in microbial ecology and ecosystem environment dynamics can be drawn.

The Middle Marker volcaniclastic platform deposits record cycles of volcanic activity and variable associated hydrothermal fluid influence as determined by major and trace element geochemistry (Fig. 5) and this system hosted photosynthetic and presumably chemosynthetic micro organisms. These shallow water deposits record offshore to shelfal supra tidal depositional conditions on the regional to local scale wherein, on the microbial scale, phototrophs colonised all available bedding plane surfaces. Textural evidence for hydrothermal input is documented not only by the pervasive silicification of the sediments but also by soft sediment de formation features produced by forceful infiltration parallel to the soft, cohesive biofilm layers, generating elongate, pod like structures (e.g. Fig. 11). Because of rapid silicification, there is little to no compaction of the delicate microbial biofilms. Thus, the varying thicknesses of the pho totrophic biofilms testify to varying sedimentation rates: where sedi mentation rates are low or zero, the thickness of the biofilm packets is higher, reaching up to several millimetres (e.g. Fig. 10D,E). Higher sedi mentation rates during depositional regimes, on the other hand, over whelm the biofilms and the packets of individual laminae are on the order of only tens of microns in thickness.

One of the striking features of the Middle Marker sedimentary environment and its microbial communities is the similarity with other volcaniclastic platform deposits in the Early Archaean. The 3.33 Ga Josefsdal Chert (equivalent to unit K1c of the Kromberg Formation; Lowe and Byerly, 1999), is a similarly widespread platform deposit, albeit at times much thicker than the Middle Marker owing to growth fault control of the depositional basin (Westall et al., 2015). Sedimentologically, it also documents a shallowing upward cycle culminating in supratidal deposits with variable current and wave influence. However, while the large felsic component of the Middle Marker indicates the waning phase of a volcanic cycle, the overwhelmingly basaltic compositions of the volcanic clasts of the Josefsdal Chert document an earlier phase of volcanism. Microbial mats and other biofabrics are similarly common in the Middle Marker and Josefsdal Chert. Further to this, Tice and Lowe (2004, 2006) and Greco et al. (2018) de scribed phototrophic biofilms from platform deposits recording a similar palaeoenvironmental setting in the 3.42 Ga Buck Reef Chert. Westall et al. (2006, 2011) investigating felsic/basaltic shallow water deposits in the 3.45 Ga Kitty's Gap Chert of the Pilbara also documented phototrophic biofilm remnants, and delicate chemolithotrophic colonies at the surfaces of volcanic clasts. Finally, Hickman Lewis et al.(2016) described probable microbial fabrics in shallow water, micro clastic cherts in the vicinity of hydrothermal activity in the 3.46 Ga stratiform 'Apex chert' at Chinaman Creek.

There is a striking similarity in the facies biocoenosis associations of these units, outlined in Table 3. Facies 1 of the Middle Marker and Facies A of the Josefsdal Chert are both characterised by coarser vol canogenic sandstones deposited in upper offshore to shoreface en vironments, and can be compared to Microfacies I of the Buck Reef Chert and the voluminous silicified volcaniclastics in the stratiform 'Apex chert'. Facies 2 of the Middle Marker, black, carbonaceous, clotted cherts are the equivalent of Facies C in the Josefsdal Chert, both facies being influenced by heat probably of hydrothermal and diage netic origin; this is evident both from their REE + Y patterns and Raman I_D/I_G intensity ratios. A comparison here can be made to clotted carbonaceous cherts in the stratiform 'Apex chert'. Facies 3 in the Middle Marker comprises finely layered green grey cherts representing mostly ashfall with minor current reworking. This facies is comparable

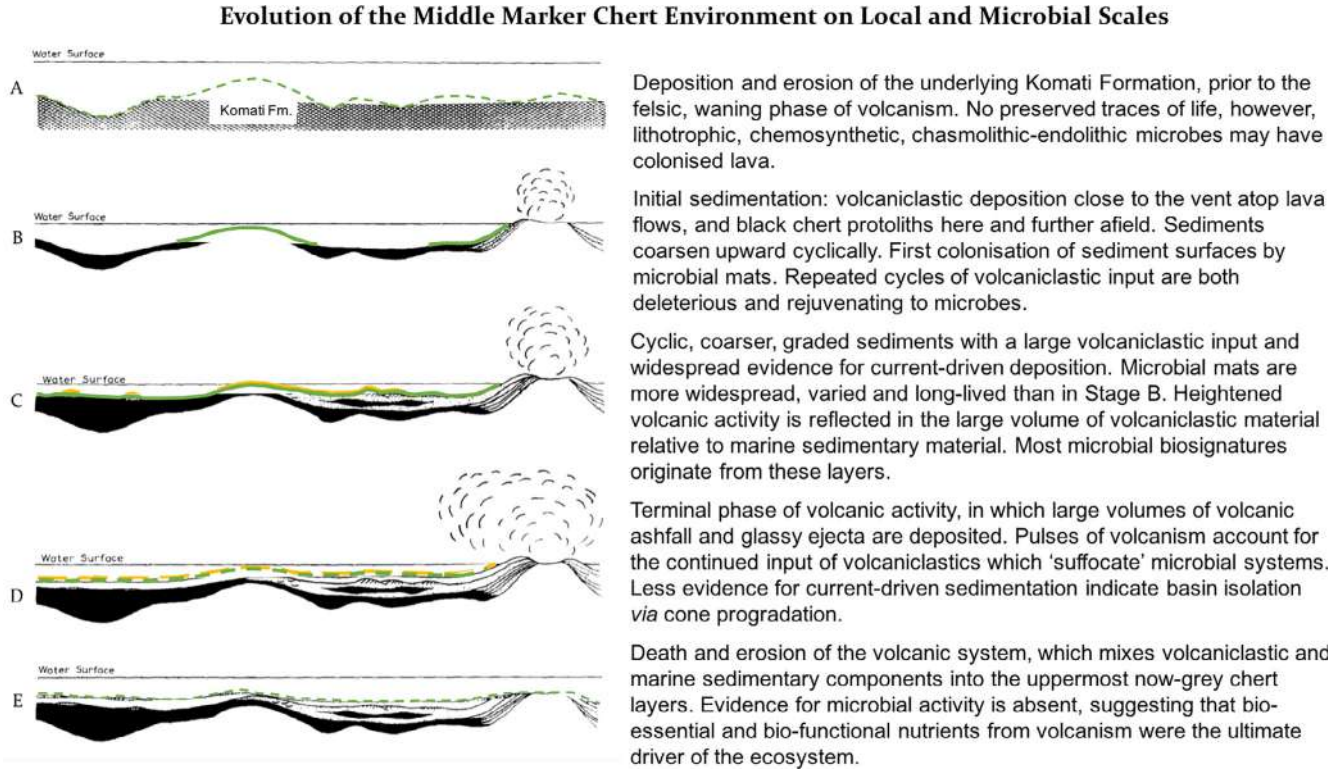

Fig. 17. Co-evolution of the environment of the Middle Marker chert and its microbial inhabitants. Though not preserved, there were possibly chemosynthetic ecosystems flourishing in the seafloor komatiites (the cryptoendolithic biosphere) prior to, and following, volcaniclastic sedimentation in the basin. Life has an apparent dependency on the nutrients provided by volcanism.

Table 3
Comparison of Palaeoarchaean shallow-water biocoenoses.

Location	Middle Marker horizon (3.472 Ga)	Josefsdal Chert (3.33 Ga)	Buck Reef Chert (3.42 Ga)	Stratiform 'Apex chert' (3.46 Ga)
Depositional Environment	Shallow-water platform, shallowing up sequence; variable current influence	Shallow-water platform, shallowing up sequence; variable current/wind influence	Deepening up sequence with major shallow platformal section	Shallow-water platform with variable current influence
Main lithology	Mafic, felsic + some komatiitic	Basaltic + some felsic	Mafic and felsic	Mafic (basaltic) and felsic
Facies	1: Coarse volcaniclastic sandstone	Facies A: coarse basaltic sandstone	Microfacies I: high clastic component, volcaniclastic and carbonaceous sediment	~ Silicified volcaniclastics
	2: Massive black clotted carbonaceous chert	Facies C: black clotted carbonaceous chert	Microfacies II: simple and complex carbonaceous grains with little clastic component	Clotted carbonaceous chert
	3: Laminated green-grey siltstones and sandstones, alternating with carbonaceous microbial biofilms	Facies D: Finely laminated green-grey siltstones and sandstones alternating with carbonaceous layers Facies B: Great thicknesses of phototrophic biofilms	Microfacies III: complex and simple carbonaceous grains with microbial mats Microfacies III, platformal facies with great thicknesses of microbial biofilms	Microclastic chert and banded black-grey-white chert with rare carbonaceous lamination ? Laminated metalliferous cherts
Hydrothermal activity	Locally present, minor component in laminated chert	Ubiquitous; locally predominant	Controversial; probably present in some facies	Ubiquitous; multiple traceable black chert veins – terminating within laminated chert – along strike
Phototrophic biofilms	Widespread in Facies 3, rare in Facies 1, absent in Facies 2	Occur in all sedimentary facies	Widespread in Microfacies III	Probable eroded clasts of microbial-like structures in microclastic cherts
Chemotrophic microfossils	If present, limited to those localities interpreted as close to hydrothermal effusions	Limited to localities close to hydrothermal vents		If present, filament-like horizons interpreted as microbial in microclastic cherts

to Facies D of the Josefsdal Chert and to microbial horizons in Hoog genoeg formation chert H5c (Walsh, 1992), the main difference being that the black carbonaceous layers in the latter are much thinner than in the former, a difference probably related to sedimentation rate.

In terms of microbial biosignatures, probable photosynthetic and chemosynthetic biofilms occur throughout these cherts. Photosynthetic or ganisms required access to sunlight, which was amply provided by their shallow water setting, their carbon sourced from dissolved CO_2 in seawater. Mixed colonies of phototrophs and chemotrophs presumably occurred close to hydrothermal vents, supported by correlative evidence between multiple chert units (Table 3). Despite the compositional differences be tween the felsic mafic Middle Marker horizon, 'Apex chert' and Buck Reef Chert and the mostly mafic Josefsdal Chert, comparable biosignatures suggest that similar microbial consortia inhabited different chert types. Photosynthetic biofilms, however, are most widespread in the Middle Marker and Buck Reef Chert. Whereas relatively low sedimentation rates in Facies 3 of the Middle Marker favoured the development of mm to cm scale phototrophic biofilms, the higher sedimentation rates of Facies D in the Josefsdal Chert (*cf*. Westall et al., 2015, see Table 3) resulted in poorly developed biofilms. This indicates that the distribution and success of mi crobial biomes is governed by both geochemical and mechanical hydro dynamic parameters.

Preservation of the microbial biosignatures was due to early silicification. Very high concentrations of silica in pore waters contributed to rapid silicification and preservation of the inorganic and the organic components of the sediments (see Westall et al., 2018). In the coarser grained facies, higher sedimentation rates entail more poorly devel oped, and poorly preserved, phototrophic biofilms. Approximately 170 Ma separates the oldest (Middle Marker) and youngest (Josefsdal Chert) of the chertified sediments compared here, yet the sedimento logical features, facies, environmental conditions and microbial in habitants throughout all are equivalent.

The biosignatures of the Middle Marker document that microbial life was already thriving in shallow water, platformal volcaniclastic sediments by 3.472 Ga. Salient similarities with comparable shallow water sediments and their microbial inhabitants in contemporaneous and younger horizons spanning the Early Archaean world paint a picture of an early Earth teeming with microbial life.

8. Conclusions

The ~3.47 Ga Middle Marker horizon is the oldest chert unit in the Barberton greenstone belt. It is a sequence of layered mafic and felsic volcaniclastic deposits with a proximal volcanic source. Sedimentary structures within indicate water depths of up to tens of metres, while soft sediment deformation is in response to synsedimentary intrusion by percolating, penetrative stratiform silica veins. Thus, the Middle Marker is interpreted to have deposited on a shallow water volcanic hydrothermal shelf. A number of laminated structures in the Middle Marker sediments bear remarkable resemblance to microbial mat textures from con- temporaneous and younger sediments from similar palaeoenvironments, and the thorough assessment of biogenicity conducted herein strongly supports the biological interpretation of kerogenous mat like laminations.

Biogenic origins are evident for crinkly, filament like laminations and pseudo tufted laminations. Isolated carbonaceous wisps and flake like particles are probable biosignatures, interpreted as the eroded remnants of crinkly, filament like laminations on the basis of spatial occurrence and equivalent dimensions. All of these structures exhibit micron scale morphological characters typical of microbial mats and evidence in sediment cohesiveness which corroborates *in vivo* plasticity.

Randomly distributed lenticular objects, directly comparable to similar features interpreted as *bona fide* microfossils in Early Archaean sediments, are a further enigmatic microstructure. In the Middle Marker horizon, the distribution of these objects, both within primary and secondary chert fabrics, within and outside of microbial mats, and encompassing a wide range of sizes, mineralogies and taphonomies, does

not support their biological interpretation. Though a wealth of data in support of the biological origins of such structures has been reported (structures whose veracity we do not here challenge), the lenticular objects in this study appear to be either ordinary detrital particles within the microbial mats, or mineralogical features unrelated to any specific sedimentary fabric, and thus of abiotic origin.

The Middle Marker horizon preserves a record of early prokaryotic diversity on Earth. A consortium of photosynthetic and probably associated chemosynthetic microbes flourished in these shallow waters, their success seemingly tied to volcaniclastic input from volcanic pulses: each flux provides the necessary bio essential elements for catalysing primitive metabolisms, as evidenced by the rapid colonisation of the tops of volcano sedimentary layers. By contrast, volcanogenic input spells destruction for the microbial ecosystem when deposited in larger volume atop a successful mat building community. Thus, volca nogenic material provides both the geochemical impetus to foster mi crobial growth and the physical mechanical hydrodynamic constraints that destroy microbial ecosystems. The shallow water, volcaniclastic biocoenosis of Archaean life was therefore one characterised by mi crobial struggle: the ecosystem flourished in times of erosion, and perished in times of deposition. This biocoenosis appears to have been common and widespread on the Archaean Earth, and facies biocoenosis similarities across such units are evident. The biofabrics of the Middle Marker are the most ancient evidence for life in the Barberton green stone belt, and the second oldest convincing evidence for life on Earth.

Acknowledgements

We are grateful to Giorgio Gasparotto (BiGeA Bologna) and Pascale Gautret (ISTO Orléans) for assistance with SEM work. Thin sections were made by Sylvain Janiec (ISTO Orléans). We acknowledge financial support for this work from the French Space Agency (CNES), the French National Centre for Scientific Research (CNRS) the MASE (Mars Analogues for Space Exploration) project (EU FP7 Grant no. 607297), and the INACMa (Inorganic Nanoparticles in Archaean Carbonaceous Matter a key to early life and palaeoenvironmental reconstructions) project (EU FP7 Grant no. 618657). KHL received support from the COST Origins Action in the form of Grant no. TD1308 37679.

References

Altermann, W., Kazmierczak, J., 2003. Archean microfossils: a reappraisal of early life on Earth. Res. Microbiol. 154, 611–617.
Anhaeusser, C.R., 1973. The evolution of the early Precambrian crust of southern Africa. Philos. Trans. R. Soc. Lond. Ser. A 273, 359–388.
Anhaeusser, C.R., 1978. The geology and geochemistry of the Muldersdrif Complex and surrounding area, Krugersdorp District. Trans. Geol. Soc. S. Afr. 81, 193–203. Armstrong, R.A., Compston, W., de Wit, M.J., Williams, I.S., 1990. The stratigraphy of 3.5-3.2 Ga barberton greenstone belt revisited: a single zircon microprobe study. Earth Planet. Sci. Lett. 101, 90–106.
Arndt, N.T., Nisbet, E.G., 2012. Processes on the young Earth and the habitats of early life. Annu. Rev. Earth Planet. Sci. 40, 521–549.
Bailey, J., Orphan, V., Joye, S., Corsetti, F., 2009. Chemotrophic microbial mats and their potential for preservation in the rock record. Astrobiology 9, 843–859.
Banerjee, N.R., Furnes, H., Meuhlenbachs, K., Staudigel, H., de Wit, M.J., 2006. Preservation of ca. 3.4–3.5 Ga microbial biomarkers in pillow lavas and hyaloclastites from the Barberton Greenstone Belt, South Africa. Earth Planet. Sci. Lett. 241, 707–722.
Barghoorn, E.S., Schopf, J.W., 1966. Microorganisms three billion years old from the Precambrian of South Africa. Science 152, 758–763.
Batustuzzi, F.A., Feijao, A., Blair Hedges, S., 2004. A genomic timescale of prokaryote evolution: insights into the origin of methanogenesis, phototrophy, and the colonization of land. BMC Evol. Biol. 4, 44.
Bau, M., Dulski, P., 1996. Distribution of yttrium and rare-earth elements in the Penge and Kuruman iron-formations, Transvaal Supergroup, South Africa. Precambrian Res. 79, 37–55.
Bosak, T., Liang, G., Sim, M.S., Petroff, A.P., 2009. Morphological record of oxygenic photosynthesis in conical stromatolites. Proc. Natl. Acad. Sci. U.S.A. 106, 10939–10943.
Bosak, T., Knoll, A.H., Petroff, A.P., 2013. The meaning of stromatolites. Annu. Rev. Earth Planet. Sci. 41, 21–44.
Bourbin, M., Gourier, D., Derenne, S., Binet, L., Le Du, Y., Westall, F., Kremer, B., Gautret, P., 2013. Dating carbonaceous matter in archean cherts by electron paramagnetic resonance. Astrobiology 13, 151–162.
Brasier, M.D., Green, O., Lindsay, J.F., Steele, A., 2004. Earth's oldest (> 3.5 Ga) fossils and the 'early Eden hypothesis': questioning the evidence. Origin Life Evol. Biosphere 34, 257–269.
Brasier, M.D., Green, O.R., Lindsay, J.F., McLoughlin, N., Steele, A., Stoakes, C., 2005. Critical testing of Earth's oldest putative fossil assemblage from the 3.5 Ga apex chert, Chinaman Creek Western Australia. Precambr. Res. 140, 55–102.
Brasier, M.D., McLoughlin, N., Green, O., Wacey, D., 2006. A fresh look at the fossil evidence for early Archaean cellular life. Philos. Trans. R. Soc. Lon. B Biol. Sci. 361, 887–902.
Brasier, M.D., Wacey, D., McLoughlin, N., 2011. Taphonomy in temporally unique settings: an environmental traverse in search of the earliest life on Earth. In: Allison, P.A., Bottjer, D.J. (Eds.), Taphonomy: Process and Bias Through Time, Topics in Geobiology. Springer, pp. 487.
Brasier, M.D., Matthewman, R., McMahon, S., Kilburn, M.R., Wacey, D., 2013. Pumice from the ~3460 Ma Apex Basalt, Western Australia: a natural laboratory for the early biosphere. Precambr. Res. 224, 1–10.
Buick, R., Dunlop, J., Groves, D., 1981. Stromatolite recognition in ancient rocks: an appraisal of irregularly laminated structures in an Early Archean chert-barite unit from North Pole, Western Australia. Alcheringa 5, 161–181.
Buick, R., 1984. Carbonaceous filaments from North Pole, Western Australia: are they fossil bacteria in Archean stromatolites? Precambr. Res. 24, 157–172.
Buick, R., 1990. Microfossil recognition in Archaean rocks: an appraisal of spheroids and filaments from 3500 M.Y. old chert-barite at North Pole, western Australia. Palaios 5, 441–459.
Busscher, H.J., Mei, H.C.V.D., 2000. Initial microbial adhesion events: mechanisms and implications. In: Allison, D.G., Gilbert, P., Lappin-Scott, H.M., Wilson, M. (Eds.), Community Structure and Co-operation in Biofilms. Cambridge University Press, Cambridge, pp. 25–36.
Byerly, G.R., Lowe, D.R., Walsh, M.M., 1986. Stromatolites from the 3300–3500 Myr Swaziland Supergroup, Barberton Mountain Land, South Africa. Nature 319, 489–491.
Cavalazzi, B., 2007. Chemotrophic filamentous microfossils from the hollard mound (Devonian, Morocco) as investigated by focused ion beam. Astrobiology 7, 402–415.
Cavalazzi, B., Barbieri, R., Ori, G.G., 2007. Chemosynthetic microbialites in the Devonian carbonate mounds of Hamar Laghdad (Anti-Atlas, Morocco). Sed. Geol. 200, 73–88.
Condie, K.C., 1981. Archean Greenstone Belts. Elsevier, Amsterdam, pp. 433p.
Dann, J.C., Grove, T.L., 2007. Volcanology of the Barberton Greenstone Belt, South Africa: inflation and evolution of flow fields. In: Van Kranendonk, M.J., Smithies, R.H., Bennett, V. (Eds.), Earth's Oldest Rocks. Developments in Precambrian Geology. Elsevier, Amsterdam, pp. 527–570.
de Wit, M.J., Hart, R.A., 1993. Earth's earliest continental lithosphere, hydrothermal flux and crustal recycling. Lithos 30, 309–335.
Decho, A.W., 1990. Microbial exopolymer secretions in ocean environments: their role(s) in food webs and marine processes. Oceanogr. Mar. Sci. Annu. Rev. 28, 73153. Decho, A.W., Kawaguchi, T., 2003. Extracellular polymers (EPS) and calcification within modern marine stromatolites. In: Krumbein, W.E., Paterson, D.M., Zavarzin, G.A. (Eds.), Fossil and Recent Biofilms. Kluwer, Dordrecht, pp. 227–240.
Delarue, F., Rouzaud, J.-N., Derenne, S., Bourbin, M., Westall, F., Kremer, B., Sugitani, K., Deldicque, D., Robert, F., 2016. The raman-derived carbonization continuum: a tool to select the best preserved molecular structures in archean kerogens. Astrobiology 16, 407–417.
Drabon, N., Lowe, D.R., Byerly, G.R., Harrington, J.A., 2017. Detrital zircon geochronology of sandstones of the 3.6–3.2 Ga Barberton greenstone belt: no evidence for older continental crust. Geology 45, 803–806.
Dziggel, A., Stevens, G., Poujol, M., Anhaeusser, C.R., Armstrong, R.A., 2002. Metamorphism of the granite-greenstone terrane south of the Barberton greenstone belt, South Africa: an insight into the tectono-thermal evolution of the 'lower' portions of the Onverwacht Group. Precambr. Res. 114, 221–247.
Dziggel, A., Stevens, G., Poujol, M., Armstrong, R.A., 2006. Contrasting source compositions of clastic metasedimentary rocks in the lowermost formations of the Barberton greenstone belt. In: Reimold, W.U., Gibson, R.L. (Eds.), Processes on the Early Earth. Geological Society of America Special Paper, pp. 157–172.
Engel, A.E.J., Nagy, B., Nagy, L.A., Engel, C.G., Kremp, G.O.W., Drew, C.M., 1968. Alga-like forms in Onverwacht Series, South Africa: oldest recognized lifelike forms on earth. Science 161, 1005–1008.
Ernst, W.G., Sleep, N.H., Tsujimori, T., 2016. Plate-tectonic evolution of the earth: bottom-up and top-down mantle circulation. Can. J. Earth Sci. 53, 1103–1120.
Flannery, D.T., Walter, M.R., 2011. Archean tufted microbial mats and the Great Oxidation Event: new insights into an ancient problem. Aust. J. Earth Sci. 59, 1–11.
Furnes, H., Banerjee, N.R., Muehlenbachs, K., Staudigel, H., de Wit, M.J., 2004. Early life recorded in Archean pillow lavas. Science 304, 578–581.
Furnes, H., Banerjee, N.R., Staudigel, H., Muehlenbachs, K., de Wit, M.J., McLoughlin, N., Van Kranendonk, M.J., 2007. Bioalteration textures in recent to mesoarchean pillow lavas: a petrographic signature of subsurface life in oceanic igneous rocks. Precambr. Res. 158, 156–176.
Gamper, A., Heubeck, C., Demskec, D., 2012. Composition and microfacies of Archean microbial mats (Moodies Group, ca. 3.22 Ga, South Africa). In: Noffke, N., Chafetz, H. (Eds.), Microbial Mats in Siliciclastic Depositional Systems Through Time. SEPM Special Publication, pp. 65–74.
Gerdes, G., 2007. Structures left by modern microbial mats in their host sediments. In: Schieber, J., Bose, P.K., Eriksson, P.G., Banerjee, S., Sarkar, S., Altermann, W., Catuneanu, O. (Eds.), Atlas of Microbial Mat Features Preserved within the Siliciclastic Rock Record. Elsevier, Amsterdam.
Gerdes, G., Krumbein, W., 1987. Biolaminated Deposits. Springer-Verlag, Berlin.
Gerdes, G., Krumbein, W.E., Reineck, H.E., 1991. Biolaminations – ecological versus

depositional dynamics. In: Einsele, G., Ricken, W., Seilacher, A. (Eds.), Cycles and events in stratigraphy. Springer, Berlin, pp. 592–607.
Gerdes, G., Noffke, N., Klenke, Th., 2000. Microbial biosignatures in peritidal siliciclastic sediments: a catalogue. Sedimentology 47, 279–308.
Gíslason, S.R., Oelkers, E.H., 2003. Mechanism, rates and consequences of basaltic glass dissolution: II. An experimental study of the dissolution rates of basaltic glass as a function of pH and temperature. Geochim. Cosmochim. Acta 67, 3817–3832. Golubic, S., 1976. Organisms that build stromatolites. In: Walter, M.R. (Ed.), Stromatolites. Elsevier, Amsterdam, pp. 113–126.
Gourcerol, B., Thurston, P.C., Kontak, D.J., Côté-Mantha, O., 2015. Interpretations and implications of LA ICP-MS analysis of chert for the origin of geochemical signatures in banded iron formations (BIFs) from the Meadowbank gold deposit, Western Churchill Province, Nunavut. Chem. Geol. 410, 89–107.
Gourcerol, B., Thurston, P.C., Kontak, D., Côté-Mantha, O., Biczok, J., 2016. Depositional setting of Algoma-type banded iron formation. Precambrian Res. 281, 47–79.
Grassineau, N.V., Nisbet, E.G., Fowler, C.M.R., Bickle, M.J., Lowry, D., Chapman, H.J., Mattey, D.P., Abell, P., Yong, J., Martin, A., 2002. Stable isotopes in the Archaean Belingwe belt, Zimbabwe: Evidence for a diverse microbial mat ecology. In: Fowler, C.M.R., Ebinger, C.J., Hawkesworth, C.J. (Eds.), The early Earth: Physical, chemical and biologi- cal development. Geological Society of London Special Publication, pp. 309–328.
Greco, F., Cavalazzi, B., Hofmann, A., Hickman-Lewis, K., 2018. 3.4 Ga biostructures from the Barberton greenstone belt of South Africa: new insights into microbial life. Bolletino della Società Paleontologica Italiana. (in press).
Grey, K., Sugitani, K., 2009. Palynology of archean microfossils (c. 3.0 Ga) from the Mount Grant area, Pilbara Craton, Western Australia: further evidence of biogenicity. Precambr. Res. 173, 60–69.
Grosch, E.G., Hazen, R.M., 2015. Microbes, mineral evolution, and the rise of micro-continents—origin and coevolution of life with early earth. Astrobiology 15, 922–939.
Harazim, D., Callow, R.H.T., McIlroy, D., 2013. Microbial mats implicated in the generation of intrastratal shrinkage (synaeresis) cracks. Sedimentology 60, 1621–1638.
Heubeck, C., 2009. An early ecosystem of Archean tidal microbial mats (Moodies Group, South Africa, ca. 3.2 Ga). Geology 37, 931–934.
Hickman-Lewis, K., Garwood, R.J., Brasier, M.D., Goral, T., Jiang, H., McLoughlin, N., Wacey, D., 2016. Carbonaceous microstructures of the 3.46 Ga stratiform 'Apex chert', Chinaman Creek locality, Pilbara Western Australia. Precambr. Res. 278, 161–178.
Hickman-Lewis, K., Garwood, R.J., Withers, P.J., Wacey, D., 2017. X-ray micro-tomography as a tool for investigating the petrological context of Precambrian cellular remains. In: Brasier, A.T., McLoughlin, N., McIlroy, D. (Eds.), Earth System Evolution and Early Life: A Celebration of the Work of Martin Brasier. Geological Society of London Special Publication, pp. 33–56.
Hickman-Lewis, K., Westall, F., Cavalazzi, B., accepted. Traces of early life from the Barberton greenstone belt, South Africa. In Van Kranendonk, M.J., Bennett, V.C., Hofmann, J.E. (Eds.) Earth's Oldest Rocks. Elsevier, Amsterdam.
Hofmann, A., 2005. The geochemistry of sedimentary rocks from the Fig Tree Group, Barberton greenstone belt: Implications for tectonic, hydrothermal and surface pro-cesses during mid-Archaean times. Precambrian Res. 143, 23–49.
Hofmann, A., 2011. Archaean hydrothermal systems in the Barberton greenstone belt and their significance as a habitat for early life. In: Golding, S.D., Glikson, M. (Eds.), Earliest Life on Earth: Habitats, Environments and Methods of Detection. Springer, Netherlands, pp. 51–78.
Hofmann, A., Bolhar, R., 2007. The origin of carbonaceous cherts in the Barberton greenstone belt and their significance for the study of early life in mid-Archean rocks. Astrobiology 7, 355–388.
Hofmann, A., Wilson, A.H., 2007. Silicified basalts, bedded cherts and other sea floor alteration phenomena of the 3.4 Ga Nondweni greenstone belt, South Africa. In: Van Kranendonk, M.J., Smithies, R.H., Bennett, V.H. (Eds.), Earth's Oldest Rocks. Elsevier (Developments in Precambrian Geology), Amsterdam, pp. 570–605.
Hofmann, A., Harris, C., 2008. Stratiform alteration zones in the Barberton greenstone belt: a window into subseafloor processes 3.5 to 3.3 Ga ago. Chem. Geol. 257, 224–242.
Hofmann, A., Bolhar, R., Orbrger, B., Foucher, F., 2013. Cherts of the Barberton Greenstone Belt, South Africa: Petrology and trace-element geochemistry of 3.5 to 3.3 Ga old silicified volcaniclastic sediments. S. Afr. J. Geol. 116, 297–322.
Homann, M., Heubeck, C., Airo, A., Tice, M.M., 2015. Morphological adaptations of 3.22 Ga tufted microbial mats to Archean coastal habitats (Moodies Group, Barberton Greenstone Belt, South Africa). Precambr. Res. 266, 47–64.
Homann, M., Heubeck, C., Bontognali, T.R.R., Bouvier, A.-S., Baumgartner, L.P., Airo, A., 2016. Evidence for cavity-dwelling microbial life in 3.22 Ga tidal deposits. Geology 44, 51–54.
House, C.H., Oehler, D.Z., Sugitani, K., Mimura, K., 2013. Carbon isotopic analyses of ca. 3.0 Ga microstructures imply planktonic autotrophs inhabited Earth's early oceans. Geology 41, 651–654.
Hurley, P.M., Pinson Jr., W.H., Nagy, B., Teska, T.M., 1972. Ancient age of the Middle Marker horizon, Onverwacht Group, Swaziland Sequence, South Africa. Earth Planet. Sci. Lett. 14, 360–366.
Javaux, E.J., Marshall, C.P., Bekker, A., 2010. Organic-walled microfossils in 3.2-billion-year-old shallow-marine siliciclastic deposits. Nature 463, 934–938.
Kamber, B.S., Greig, A., Collerson, K.D., 2005. A new estimate for the composition of weathered young upper continental crust from alluvial sediments, Queensland, Australia. Geochim. Cosmochim. Acta 69, 1041–1058.
Kempe, S., Degens, E.T., 1985. An early soda ocean? Chem. Geol. 53, 95–108. Knauth, L.P., 2005. Temperature and salinity history of the Precambrian ocean: I mplications for the course of microbial evolution. Palaeogeogr. Palaeoclimatol. Palaeoecol. 219, 53–69.
Knoll, A.H., Barghoorn, E.S., 1977. Archean microfossils showing cell division from the Swaziland System of South Africa. Science 189, 396–398.
Knoll, A.H., Strother, P.K., Rossi, S., 1988. Distribution and diagenesis of microfossils from the Lower Proterozoic Duck Creek Dolomite, Western Australia. Precambr. Res. 38, 257–279.
Kremer, B., Kazmierczak, J., 2017. Cellularly preserved microbial fossils from ~3.4 Ga deposits of South Africa: a testimony of early appearance of oxygenic life? Precambr. Res. 295, 117–129.
Lanier, W.P., Lowe, D.R., 1982. Sedimentology of the Middle Marker (3.4Ga), Onverwacht Group, Transvaal, South Africa. Precambr. Res. 18, 237–260.
Lespade, P., Al-Jishi, R., Dresselhaus, M.S., 1982. Model for Raman scattering from incompletely graphitized carbons. Carbon 20, 427–431.
Lowe, D.R., 1999a. Petrology and sedimentology of cherts and related silicified sedimentary rocks in the Swaziland Supergroup. In: Lowe, D.R., Byerly, G.R. (Eds.), Geologic Evolution of the Barberton Greenstone Belt, South Africa. Geological Society of America Special Paper, pp. 83–114.
Lowe D.R., 1999b. Geologic evolution of the Barberton Greenstone Belt and vicinity. In Lowe, D.R., Byerly, G.R. (Eds.) Geologic evolution of the Barberton Greenstone Belt, South Africa. Geological Society of America Special Paper 329, pp. 287–312. Lowe, D.R., Knauth, L.P., 1977. Sedimentology of the Onverwacht Group (3.4 billion years), Transvaal, South Africa, and its bearing on characteristics and evolution of early Earth. J. Geol. 85, 699–723.
Lowe, D.R., Knauth, L.P., 1978. The oldest marine carbonate ooids reinterpreted as volcanic accretionary lapilli: Onverwacht Group, South Africa. J. Sediment. Petrol. 48, 709–722.
Lowe, D.R., Byerly, G.R., 1999. Stratigraphy of the west-central part of the Barberton Greenstone Belt, South Africa. In: Lowe, D.R., Byerly, G.R. (Eds.), Geologic evolution of the Barberton Greenstone Belt, South Africa. Geological Society of America Special Paper, pp. 1–36.
Lowe, D.R., Byerly, G.R., 2007. An overview of the geology of the Barberton Greenstone Belt and vicinity: implications for early crustal development. In: Van Kranendonk, M.J., Smithies, R.H., Bennett, V.H. (Eds.), Earth's Oldest Rocks. Elsevier (Developments in Precambrian Geology), Amsterdam, pp. 481–526.
Maliva, R.G., Knoll, A.H., Simonson, B.M., 2005. Secular change in the Precambrian silica cycle: insights from chert petrology. Geol. Soc. Am. Bull. 117, 835–845.
Margulis, L., Barghoorn, E.S., Ashendorf, D., Banerjee, S., Chase, D., Francis, S., Giovannoni, S., Stolz, J., 1983. The microbial community in the layered sediments at Laguna Fugueroa, Baja California, Mexico: does it have Precambrian analogues? Precambr. Res. 11, 93–123.
Marshall, C.P., Love, G.D., Snape, C.E., Hill, A.C., Allwood, A.C., Walter, M.R., Van Kranendonk, M.J., Bowden, S.A., Sylva, S.P., Summons, R.E., 2007. Structural characterization of kerogen in 3.4 Ga Archaean cherts from the Pilbara Craton, Western Australia. Precambr. Res. 155, 1–23.
McCollum, T.M., Amend, J.P., 2005. A thermodynamic assessment of energy requirements for biomass synthesis by chemolithoautotrophic micro-organisms in oxic and anoxic environments. Geobiology 3, 135–144.
Monty, C.L.V., 1976. The origin and development of cryptalgal fabrics. In: Walter, M.R. (Ed.), Stromatolites. Elsevier, Amsterdam, pp. 193–249.
Muir, M.D., Grant, P.R., 1976. Micropaleontological evidence from the Onverwacht Group, South Africa. In: Windley, B.F. (Ed.), The Early History of the Earth. Wiley-lnterscience, London, pp. 595–608.
Nagy, B., Nagy, L.A., 1969. Early Precambrian Onverwacht microstructures: possibly the oldest fossils on earth? Nature 223, 1226–1229.
Neu, T.R., Eitner, A., Paje, M.L., 2003. Development and architecture of complex environmental biofilms. In: Krumbein, W.E., Paterson, D.M., Zavarzin, G.A. (Eds.), Fossil and Recent Biofilms. Kluwer, Dordrecht, pp. 29–45.
Nisbet, E.G., 2000. The realms of Archaean life. Nature 405, 625–626.
Nisbet, E.G., Fowler, C.M.R., 1996. The early history of life. Geological Society of London Special Publication, pp. 239–251.
Nisbet, E.G., Sleep, N.H., 2001. The habitat and nature of early life. Nature 409, 1083–1091.
Noffke, N., 2003. Epibenthic cyanobacterial communities interacting with sedimentary processesi siliciclastic depositional systems (present and past). In: Krumbein, W.E., Paterson, D.M., Zavarzin, G.A. (Eds.), Fossil and Recent Biofilms. Kluwer, Dordrecht, pp. 265–280.
Noffke, N., 2009. The criteria for the biogenicity of microbially induced sedimentary structures (MISS) in Archean and younger, sandy deposits. Earth Sci. Rev. 96, 173–180.
Noffke, N., 2010. Geobiology: Microbial Mats in Sandy Deposits from the Archaean Era to Today. Springer-Verlag, Berlin, Heidelberg.
Noffke, N., Gerdes, G., Klenke, T., Krumbein, W.E., 2001. Microbially induced sedimentary structures – a new category within the classification of primary sedimentary structures: perspectives. J. Sediment. Res. 71, 649–656.
Noffke, N., Hazen, R.M., Nhleko, N., 2003. Earth's earliest microbial mats in a siliciclastic marine environment (2.9 Ga Mozaan Group, South Africa). Geology 31, 673–676. Noffke, N., Eriksson, K.A., Hazen, R.M., Simpson, E.L., 2006a. A new window into Archean life: Microbial mats in Earth's oldest siliciclastic tidal deposits (3.2 Ga Moodies Group, South Africa). Geology 34, 253.
Noffke, N., Beukes, N., Gutzmer, J., Hazen, R.M., 2006b. Spatial and temporal distribution of microbially induced sedimentary structures: a case study from siliciclastic storm deposits of the 2.9 Ga Witwatersrand Supergroup South Africa. Precambr. Res. 146, 35–44.
Noffke, N., Christian, D., Wacey, D., Hazen, R.M., 2013. Microbially induced sedimentary structures recording an ancient ecosystem in the ca. 3.48 billion- year-old Dresser Formation, Pilbara Western Australia. Astrobiology 13, 1103–1124.

Oehler, D.Z., Robert, F., Walter, M.R., Sugitani, K., Allwood, A., Meibom, A., Mostefaoui, S., Selo, M., Thomen, A., Gibson, E.K., 2009. NanoSIMS: insights to biogenicity and syngeneity of Archaean carbonaceous structures. Precambr. Res. 173, 70–78.

Oehler, D.Z., Walsh, M.M., Sugitani, K., Liu, M.-C., House, C.H., 2017. Large and robust lenticular microorganisms on the young Earth. Precambr. Res. 296, 112–119.

Oelkers, E.H., Gíslaison, S.R., 2001. The mechanism, rates, and consequences of basaltic glass dissolution: I. An experimental study of the dissolution rates of basaltic glass as a function of aqueous Al, Si, and oxalic acid concentration at 25°C and pH = 3 and 11. Geochim. Cosmochim. Acta 65, 3671–3681.

Oschmann, W., 2000. Microbes and black shales. In: Riding, R.E., Awramik, S.M. (Eds.), Microbial Sediments. Springer-Verlag, Berlin Heidelberg, pp. 137–148.

Paris, I.A., Stanistreet, I.G., Hughes, M.J., 1985. Cherts of the Barberton greenstone belt interpreted as products of submarine exhalative activity. J. Geol. 93, 111–129. Parkes, R.J., Cragg, B., Roussel, E., Webster, G., Weightman, A., Sass, H., 2014. A review of prokaryotic populations and processes in sub-seafloor sediments, including biosphere:geosphere interactions. Mar. Geol. 352, 409–425.

Paterson, D.M., Yates, M.G., Wiltshire, K.H., McGrorty, S., Miles, A., Eastwood, J.E.A., Blackburn, J., Davidson, I., 1998. Microbial mediation of spectral reflectance from intertidal cohesive sediments. Limnol. Oceanogr. 43, 1207–1221.

Paterson, D.M., Perkins, R., Consalvey, M., Underwood, G.J.C., 2003. Ecosystem function, cell microcycling and the structure of transient biofilms. In: Krumbein, W.E., Paterson, D.M., Zavarzin, G.A. (Eds.), Fossil and Recent Biofilms: A Natural History of Life on Earth. Kluwer, Dodrecht, pp. 47–63.

Pflug, H.D., 1966. Organic remains from the Fig Tree Series of the Barberton Mountain Land. University of the Witwatersrand Economic Geology Research Unit, Inforomation Circular 28, Johannesburg, 36 pp.

Pope, M.C., Grotzinger, J.P., 2000. Controls on fabric development and morphology of tufa and stromatolites, uppermost Pethei Group (1.8 Ga), Great Slave Lake, northwest Canada. In: Grotzinger, J., James, N. (Eds.), Carbonate Sedimentation and Diagenesis in the Evolving Precambrian World. SEPM Special Publication, pp. 103–122.

Pope, M.C., Grotzinger, J.P., Schreiber, B.C., 2000. Evaporitic subtidal stromatolites produced by in situ precipitation: textures, facies associations, and temporal significance. J. Sediment. Res. 70, 1139–1151.

Reineck, H.E., 1967. Layered sediments of tidal flats, beaches, and shelf bottoms of the North Sea. In: G.H. Lauff (Ed.), Estuaries. American Association for the Advancement of Science Publication 83, 191–206.

Reitner, J., 2010. Architecture of archaeal-dominated microbial mats from cold seeps in the Black Sea (Dnjepr Canyon, Lower Crimean Shelf). In: Seckbach, J., Oren, A. (Eds.), Microbial Mats: Modern and Ancient Microorganisms in Stratified Systems. Springer Verlag, Heidelberg, pp. 207–220.

Revsbech, N.P., 1989. Microsensors: spatial gradients in biofilms. In Characklis, W.G., Wilderer, P.A. (Eds.) Structure and Function of Biofilms. John G. Wiley and Sons Ltd., Dahlem Konferenzen 1989, Chichester, New York, pp. 129–144.

Sadezky, A., Muckenhuber, H., Grothe, H., Niessner, R., Poschl, U., 2005. Raman microspectroscopy of soot and related carbonaceous materials: Spectral analysis and structural information. Carbon 43, 1731–1742.

Schieber, J., 1986. The possible role of benthic microbial mats during the formation of carbonaceous shales in shallow Mid-Proterozoic basins. Sedimentology 33, 521–536. Schieber, J., 1998. Possible indicators of microbial mats deposits in shales and sandstones: examples from the Mid-Proterozoic Belt Supergroup, Montana, U.S.A. Sed. Geol. 120, 105–124.

J. Schieber, J., Bose, P.K., Eriksson, P.G., Banerjee, S., Sarkar, S., Altermann, W., Catuneanu, O. (Eds.), 2007. Atlas of Microbial Mat Features Preserved within the Siliciclastic Rock Record. Elsevier, Amsterdam.

Schieber, J., Southard, J.B., Schimmelmann, A., 2012. Lenticular shale fabrics resulting from intermittent erosion of water-rich muds – interpreting the rock record in the light of recent flume experiments. J. Sediment. Res. 80, 119–128.

Schopf, J.W., 2006. Fossil evidence of Archaean life. Philos. Trans. R. Soc. Lon. B Biol. Sci. 361, 869–885.

Schopf, J.W., Walter, M.R., 1983. Archean microfossils: New evidence of ancient microbes. In: Schopf, J.W. (Ed.), Earth's Earliest Biosphere: Its Origin and Evolution. Princeton University Press, New York, pp. 214–239.

Sforna, M.C., van Zuilen, M.A., Philippot, P., 2014. Structural characterization by Raman hyperspectral mapping of organic carbon in the 3.46 billion-year-old Apex chert Western Australia. Geochim. Cosmochim. Acta 124, 18–33.

Siesser, W.G., Rogers, J., 1976. Authigenic pyrite and gypsum in south-west African Continental slope sediments. Sedimentology 23, 567–577.

Siever, R., 1992. The silica cycle in the Precambrian. Geochim. Cosmochim. Acta 56, 3265–3272.

Simonson, B.M., Schubel, K.A., Hassler, S.W., 1993. Carbonate sedimentology of the early Precambrian Hamersley Basin Group of western Australia. Precambr. Res. 60, 287–335.

Sleep, N.H., Zahnle, K., Neuhoff, P.S., 2001. Initiation of clement surface conditions on the earliest Earth. Proc. Natl. Acad. Sci. U.S.A. 98, 3666–3672.

Sugitani, K., Grey, K., Allwood, A., Nagaoka, T., Mimura, K., Minami, M., Marshall, C.P., Van Kranendonk, M.J., Walter, M.R., 2007. Diverse microstructures from Archean chert from the Mount Goldsworthy-Mount Grant area, Pilbara Craton, Western Australia: microfossils, dubiofossils, or pseudofossils? Precambr. Res. 158, 228–262.

Sugitani, K., Grey, K., Nagaoka, T., Mimura, K., 2009. Three-dimensional morphological and textural complexity of Archean putative microfossils form the northeastern Pilbara Craton: indications of biogenicity of large (> 15mm) spheroidal and spindle-like structures. Astrobiology 9, 603–615.

Sugitani, K., Lepot, K., Nagaoka, T., Mimura, K., Van Kranendonk, M.J., Oehler, D.Z., Walter, M.R., 2010. Biogenicity of morphologically diverse carbonaceous micro-structures from the ca. 3,400 Ma Strelley Pool Formation, in the Pilbara Craton, Western Australia. Astrobiology 10, 899–920.

Sugitani, K., Mimura, K., Takeuchi, M., Yamaguchi, T., Suzuki, K., Senda, R., Asahara, Y., Wallis, S., Van Kranendonk, M.J., 2015. A Paleoarchean coastal hydrothermal field inhabited by diverse microbial communities: the Strelley Pool Formation, Pilbara Craton, Western Australia. Geobiology 13, 522–545.

Sumner, D.Y., 1997. Late Archean calcite-microbe interactions: two morphologically distinct microbial communities that affects calcite nucleation differently. Palaios 12, 302–318. Sutherland, I.W., 2001. The biofilm matrix – an immobile but dynamic microbial environment. Trends Microbiol. 9, 222–227.

Tankard, A.J., Jackson, M.P.A., Eriksson, K.A., Hobday, D.K., Hunter, D.R., Minter, W.E.L., 1982. Crustal Evolution of Southern Africa, 3.8 Billion Years of Earth History. Springer-Verlag, New York, Heidelberg and Berlin.

Tartèse, R., Chaussidon, M., Gurenko, A., Delarue, F., Robert, F., 2017. Warm Archean oceans reconstructed from oxygen isotope composition of early-life remnants. Geochem. Perspect. Lett. 3, 55–65.

Tice, M.M., 2009. Environmental controls on photosynthetic microbial mat distribution on and morphogenesis on a 3.42 Ga clastic-starved platform. Astrobiology 9, 989–1000. Tice, M.M., Lowe, D.R., 2004. Photosynthetic microbial mats in the 3416-Myr-old ocean. Nature 431, 549–552.

Tice, M.M., Lowe, D.R., 2006. The origin of carbonaceous matter in pre-3.0 Ga greenstone terrains: a review and new evidence from the 3.42 Ga Buck Reef Chert. Earth Sci. Rev. 76, 259–300.

Tice, M.M., Bostick, B.C., Lowe, D.R., 2004. Thermal history of the 3.5-3.2 Ga Onverwacht and Fig Tree Groups, Barberton greenstone belt, South Africa, inferred by Raman microspectroscopy of carbonaceous material. Geology 32, 37–40.

Van Kranendonk, M.J., 2006. Volcanic degassing, hydrothermal circulation and the flourishing of early life on Earth: a review of the evidence from c. 3490–3240 Ma rocks of the Pilbara Supergroup, Pilbara Craton, Western Australia. Earth-Sci. Rev. 74, 197–240.

Van Kranendonk, M.J., 2007. A review of the evidence for putative Paleoarchean life in the Pilbara craton, Western Australia. In: Van Kranendonk, M.J., Smithies, R.H., Bennett, V.H. (Eds.), Earth's Oldest Rocks. Elsevier (Developments in Precambrian Geology), Amsterdam, pp. 855–877.

van Zuilen, M.A., Chaussidon, M., Rollion-Bard, C., Marty, B., 2007. Carbonaceous cherts of the Barberton greenstone belt, South Africa: isotopic, chemical and structural characteristics of individual microstructures. Geochim. Cosmochim. Acta 71, 655–669.

Viljoen, M.J., Viljoen, R.P., 1969. An introduction to the geology of the Barberton granite-greenstone terrain. Geol. Soc. S. Afr. Spec. Publ. 2, 9–28.

Wacey, D., 2009. Early life on earth, a practical guide. In: Landman, N.H., Harries, P.J. (Eds.), Topics in Geobiology. Springer, Heidelberg.

Walsh, M.M., 1992. Microfossils and possible microfossils from the Early Archean Onverwacht Group, Barberton Mountain Land, South Africa. Precambr. Res. 54, 271–293. Walsh, M.M., Lowe, D.R., 1985. Filamentous microfossils from the 3,500 Myr-old Onverwacht Group, Barberton Mountain Land, South Africa. Nature 314, 530–532. Walsh, M.M., Lowe, D.R., 1999. Modes of accumulation of carbonaceous matter in the early Archaean: a petrographic and geochemical study of the carbonaceous cherts of the Swaziland Supergroup. In: Lowe, D.R., Byerly, G.R. (Eds.), Geologic Evolution of the Barberton Greenstone Belt, South Africa. Geological Society of America Special Paper, pp. 115–132.

Walsh, M.M., Westall, F., 2003. Archean biofilms preserved in the Swaziland Supergroup, South Africa. In: Krumbein, W.E., Paterson, D.M., Zavarzin, G.A. (Eds.), Fossil and Recent Biofilms: A Natural History of Life on Earth. Kluwer, Dodrecht, pp. 307–316. Walter, M.R., Buick, R., Dunlop, J., 1980. Stromatolites, 3400–3500 Myr old from the North Pole area, Western Australia. Nature 284, 443–445.

Westall, F., 2016. Microbial palaeontology and the origin of life: a personal approach. Bollettino della Società Paleontologica Italiana 55, 85–103.

Westall, F., Gernecke, D., 1998. Electron microscope methods in the search for the earliest life on Earth (in 3.5–3.3 Ga cherts from the Barberton greenstone belt, South Africa): applications for extraterrestrial life studies. Proc. SPIE. Intl. Soc. Opt. Eng. 3114, 158–169.

Westall, F., Cavalazzi, B., 2011. Biosignatures in rocks. In: Thiel, V. (Ed.), Encyclopedia of Geobiology. Springer, Berlin, pp. 189–201.

Westall, F., de Wit, M.J., Dann, J., van der Gaast, S., de Ronde, C.E.J., Gerneke, D., 2001. Early Archaean fossil bacteria and biofilms in hydrothermally–influenced sediments from the Barberton greenstone belt, South Africa. Precambr. Res. 106, 93–116. Westall, F., de Ronde, C.E.J., Southam, G., Grassineau, N., Colas, M., Cockell, C.S., Lammer, H., 2006. Implications of a 3.472–3.333 Gyr-old subaerial microbial mat from the Barberton greenstone belt, South Africa for the UV environmental conditions on the early Earth. Philos. Trans. R. Soc. B Biol. Sci. 361, 1857–1875.

Westall, F., Cavalazzi, B., Lemelle, L., Marrocchi, Y., Rouzaud, J.N., Simionovici, A., Salomé, M., Mostefaoui, S., Andreazza, C., Foucher, F., Toporski, J., Jauss, A., Thiel, V., Southam, G., MacLean, L., Wirick, S., Hofmann, A., Meibom, A., Robert, F., Défarge, C., 2011. Implications of in situ calcification for photosynthesis in a ~3.3 Ga-old microbial biofilm from the Barberton Greenstone Belt, South Africa. Earth Planet. Sci. Lett. 310, 468–479.

Westall, F., Campbell, K.A., Bréhéret, J.G., Foucher, F., Gautret, P., Hubert, A., Sorieul, S., Grassineau, N., Guido, D.M., 2015. Archean (3.33Ga microbe-sediment systems were diverse and flourished in a hydrothermal context. Geology 43, 615–618.

Westall, F., Hickman-Lewis, K., Hinman, N., Gautret, P., Campbell, K.A., Bréhéret, J.-G., Foucher, F., Hubert, A., Sorieul, S., Kee, T.P., Dass, A.V., Georgelin, T., Brack, A., 2018. A hydrothermal-sedimentary context for the origin for life. Astrobiology 18, 259–293.

Williams, L.A., Reimers, C., 1982. Recognizing organic mats in deep water environments. Geol. Soc. Am. Abstracts Programs 14, 647.

Wolff-Boenisch, D., Gíslason, S.R., Oelkers, E.H., 2006. The effect of crystallinity on dissolution rates and CO2 consumption capacity of silicates. Geochim. Cosmochim. Acta 70, 858–870.